Linear Collider Vision

The Linear Collider Facility (LCF) at CERN – Back-up Document –

updated version May 26, 2025

Contact persons: Jenny List* Steinar Stapnes†

on behalf of the LCVision Editorial Board: Masaya Ishino (U. Tokyo), Benno List (DESY), Jenny List (DESY), Tatsuya Nakada (EPFL Lausanne), Michael Peskin (SLAC), Roman Pöschl (IJCLab), Aidan Robson (U. Glasgow), Thomas Schörner (DESY/CERN), Steinar Stapnes (CERN)

In this paper we outline a proposal for a Linear Collider Facility as the next flagship project for CERN. This proposal offers the opportunity for a timely, cost-effective and staged construction of a new collider that will be able to comprehensively map the Higgs boson's properties, including the Higgs field potential, thanks to a large span in centre-of-mass energies and polarised beams. A comprehensive programme to study the Higgs boson and its closest relatives with high precision requires data at centre-of-mass energies from the Z pole to at least 1 TeV. It should include measurements of the Higgs boson in both major production mechanisms, $e^+e^- \to ZH$ (Higgs-strahlung) and $e^+e^- \to \nu\bar{\nu}H$ (WW fusion), precision measurements of gauge boson interactions as well as of the W boson, Higgs boson and top-quark masses, measurement of the top-quark Yukawa coupling through $e^+e^- \to t\bar{t}H$, measurement of the Higgs boson self-coupling through HH production, and precision measurements of the electroweak couplings of the top quark. In addition, e^+e^- collisions offer discovery potential for new particles complementary to HL-LHC. The facility we propose robustly satisfies these scientific goals. With a total length of 33.5 km, two interaction regions as well as additional R&D and fixed-target experiments, it offers significant flexibility to take into account scientific and strategic developments. From today's perspective, we propose to equip the Linear Collider Facility in a first stage with superconducting RF cavities for polarised e^+e^- collisions at a centre-of-mass energy of 250 GeV with a luminosity of $2.7 \times 10^{34}\,\mathrm{cm}^{-2}\mathrm{s}^{-1}$, which requires an investment of about 8.3 BCHF. With a preparatory phase of eight years, followed by ten years of construction starting earliest in 2034, this first stage could start beam commissioning and data-taking a decade later. First upgrades comprise doubling of the luminosity for 0.8 BCHF and an increase of energy up to at least 550 GeV, which can be achieved with the same accelerator technology for about 5.5 BCHF. Later stages will involve further increase of luminosity and energy as well as other new capabilities that will further enhance the Higgs programme and extend the discovery potential for new physics. These upgrades will primarily be accomplished by accelerator technology innovations rather than by additional civil construction.

Contents

1 Stages and parameters **2**

2 Timeline **4**

3 Resource requirements **5**

3.1 Construction cost and costing methodology 5

3.2 Operating costs 10

4 Sustainability and environmental impact **11**

5 Technology and delivery **14**

5.1 Overview, R&D requirements and next steps 15

5.2 Assessment of technology readiness 16

6 Dependencies **21**

7 Commentary on current project status **21**

8 Performance Risks and Opportunities **21**

8.1 Accelerating gradient and collision energy 22

8.2 Quality factor Q_0 and cryogenic power, new surface treatments 25

8.3 Risk assessment conclusion 26

1 Stages and parameters

The main stages of the Linear Collider Project (LCF) and the key scientific goals of each are sketched in Fig. 1 for two scenarios A and B, which are defined as follows:

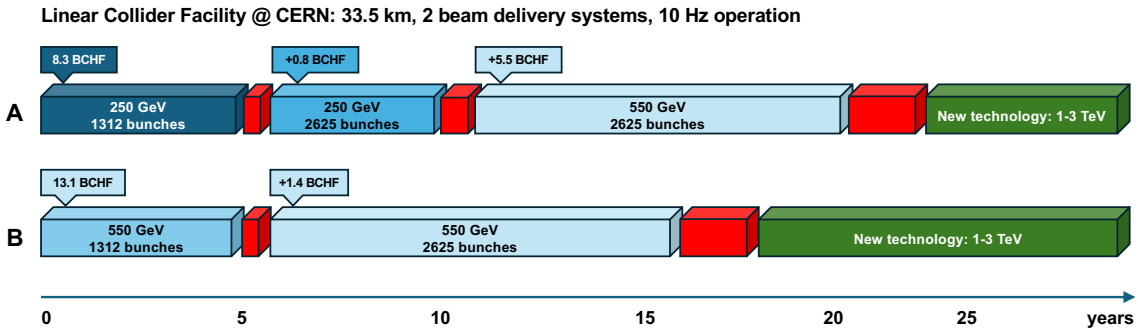

Figure 1: Visualisation of the timelines of scenarios A and B. The technical time zero would be around 2044. Note that the Linear Collider Facility offers significant flexibility to react to i) findings at or developments with other machines (HL-LHC, CEPC, ...) and to ii) the technical readiness of particular implementations.

- **Scenario A**, i.e. starting with 250 GeV, gives a large data set of $e^+e^- \to ZH$ events for measurements of Higgs branching ratios (to 1 %), the total ZH cross section (to 1 %), the absolute Higgs coupling normalisations and the Higgs boson mass (to 10^{-4} precision). It also enables searches for non-standard Higgs boson decays (to the 10^{-4} level of branching ratios), and it allows for a collection of a few 10^9 events at the Z pole.
  - The **power upgrade of scenario A** from 1312 ("low power", LP) to 2625 bunches ("full power", FP) will double the available luminosity.

Quantity	Symbol	Unit	Initial-250	Upgrades		Initial-550	Upgrade
Name		LCF	250 LP	250 FP	550 FP	550 LP	550 FP
Centre-of-mass energy	$\sqrt{s}$	GeV	250	250	550	550	550
Inst. luminosity	$\mathscr{L}$ ($10^{34} cm^{-2} s^{-1}$)		2.7	5.4	7.7	3.9	7.7
Polarisation	$\lvert P(e^-)\rvert$/ $\lvert P(e^+)\rvert$ (%)		80 / 30	80 / 30	80 / 60	80 / 30	80 / 60
Repetition frequency	f_{rep}	Hz	10	10	10	10	10
Bunches per pulse	n_{bunch}	1	1312	2625	2625	1312	2625
Bunch population	N_e	10^{10}	2	2	2	2	2
Linac bunch interval	Δt_b	ns	554	366	366	554	366
Beam current in pulse	I_{pulse}	mA	5.8	8.8	8.8	5.8	8.8
Beam pulse duration	t_{pulse}	μs	727	897	897	727	897
Average beam power	P_{ave}	MW	10.5	21	46	23	46
Norm. hor. emitt. at IP	$\gamma\varepsilon_x$	μm	5	5	10	10	10
Norm. vert. emitt. at IP	$\gamma\varepsilon_y$	nm	35	35	35	35	35
RMS hor. beam size at IP	σ_x^*	nm	516	516	452	452	452
RMS vert. beam size at IP	σ_y^*	nm	7.7	7.7	5.6	5.6	5.6
Lumi frac. in top 1 %	$\mathscr{L}_{0.01}/\mathscr{L}$	%	73	73	58	58	58
Lumi in top 1 %	$\mathscr{L}_{0.01}$ ($10^{34} cm^{-2} s^{-1}$)		2.0	4.0	4.5	2.2	4.5
Site AC power	P_{site}	MW	143	182	322	250	322
Annual energy consumption		TWh	0.8	1.0	1.8	1.4	1.8
Site length	L_{site}	km	33.5	33.5	33.5	33.5	33.5
Average gradient	g	MV/m	31.5	31.5	31.5	31.5	31.5
Quality factor	Q_0	10^{10}	2	2	2	2	2
Construction cost		BCHF	8.29	+0.77	+5.46	13.13	+1.40
Construction labour		kFTE y	10.12		+3.65	13.77	
Operation and maintenance		MCHF/y	156	182	322	273	322
Electricity		MCHF/y	66	77	142	115	142
Operating personnel		FTE	640	640	850	850	850

Table 1: Summary table of the LCF accelerator parameters in the initial 250 GeV configuration and possible upgrades, as well as in an initial 550 GeV configuration and its luminosity upgrade.

  - The **energy upgrade of scenario A** to 550 GeV will give access to WW fusion events, with an independent setting for Higgs branching ratio measurements and exotic decay searches. Importantly, it will facilitate measurements of the top quark Yukawa coupling (through $e^+e^- \to t\bar{t}H$) and of the Higgs self-coupling (through $e^+e^- \to ZHH$). It will also enable measurements of top quark properties, not least the top mass in top-pair threshold measurements.

- **Scenario B**, i.e. starting with 550 GeV, gives immediate access to all mentioned measurements in the entire energy range from the Z pole to 550 GeV.
  - The **power upgrade of scenario B**, from 1312 to 2625 bunches, will double the available luminosity.

- A later **stage at 1** TeV or beyond provides access to WW fusion to HH and thus a complementary access to the Higgs self-coupling. There will be increased sensitivity to anomalies in the top quark couplings. Ample single-Higgs production will allow for further scrutiny of the Higgs couplings to SM particles.

- An potential ultimate **stage at 3** TeV might grant access to new particles discovered or hinted to at the HL-LHC, and will give access to the quartic Higgs coupling.

The ordering and scope of stages is not fixed and allows for flexibility. Two alternative starting scenarios for the LCF, one with 250 GeV and one with 550 GeV centre-of-mass energy, are sketched

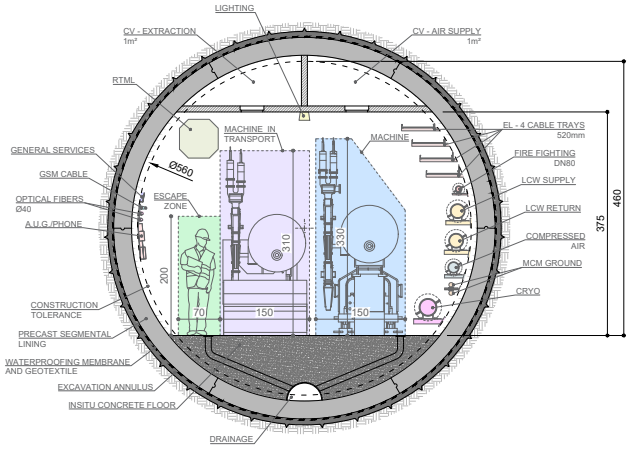

Figure 2: Cross section of the 5.6 m tunnel of a Linear Collider Facility at CERN.

above. These scenarios are interchangeable, depending e.g. on the initially available funding. There is no technical reason preventing alternative starting scenarios, for instance directly with full power (i.e. twice higher luminosity) or at an intermediate centre-of-mass energy, e.g. 380 GeV, provided sufficient initial funding can be secured. Note that thus the Linear Collider Facility in general offers significant flexibility to react to i) findings at or developments with other machines (HL-LHC, CEPC, ...) and to ii) the technical readiness of particular implementations.

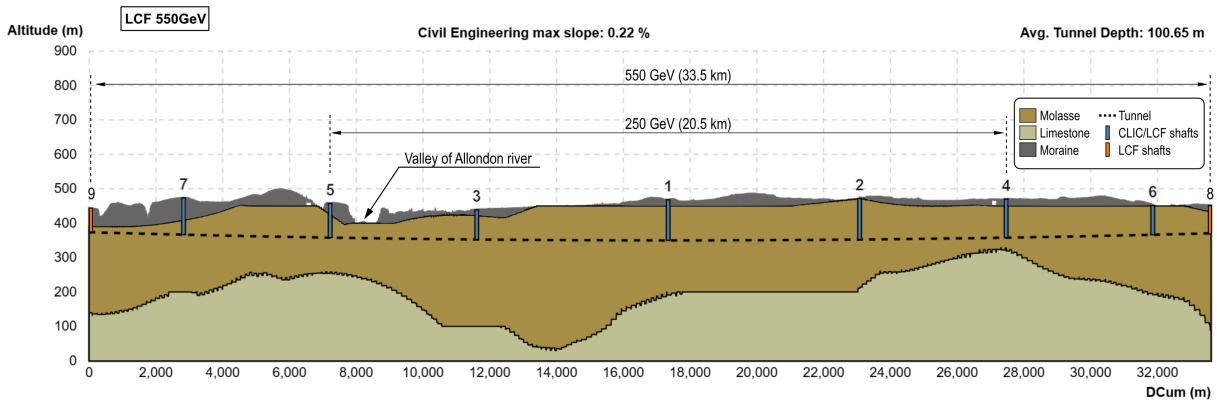

Figure 3: . Geological profile of the LCF tunnel and the location of its access shafts.

For each stage, in both scenarios, the main technical parameters are listed in Tab 1. As an important ingredient, Fig. 2 shows the tunnel cross-section of diameter 5.6 m for the Linear Collider Facility at CERN. Figure 3 shows the geological profile of the foreseen LCF tunnel location, together with the indicative shaft locations.

2 Timeline

Both scenarios A and B are essentially ready to be built (see the discussion of remaining R&D items in Sec. 5). The chosen technology – ILC-type superconducing RF – is mature and has its industrialisation has been successfully completed in the context of the European XFEL at DESY, Hamburg. A construction and site preparation time of 9 years is assumed, irrespective of the scenario. Table 2 shows the anticipated timeline for the various steps of the project in years. The definition

of project implementation phases is used as given in the main document of this submission. T_0 is determined by a process in 2028-29 to validate the progress and promise of the project for a further development towards implementation. T_1 for the start of the construction phase will be determined by the processes needed, by the CERN Council and with host-states, for project approval and to start construction. The construction phase is extended with respect to the technical schedules to allow a transfer time into construction, and to avoid the resource conflict between HL-LHC operation and initiating beam commissioning for a next collider.

Milestone	LCF@CERN
Conceptual/Reference Design Report	2002 – 2007
Technical Design Report	2007 – 2013
ILC 250 GeV reports and Prelab planning	2013 – 2025
Project Preparation Phase 1	2026 – 2028
Definition of the placement scenario	
Design optimisation and finalization	
Main technologies R&D conclusions	
Technical Design Report – two IPs at CERN	
Project Preparation Phase 2	T_0 – (T_0+5)
Site investigation and preparation	
Implementation studies with the Host states	
Environmental evaluation & project authorisation processes	
Industrialization of key components	
Engineering design completion	
Construction Phase (from ground breaking)	T_1 – (T_1+10)
Civil engineering	
Construction of components	
Installation and hardware commissioning	
Beam commissioning and physics operation start	T_1+11

Table 2: Timeline of essential development and construction steps of the LCF project. See the text for details.

The anticipated running times and envisaged integrated luminosities for scenarios A and B are indicated in Fig. 4. Note that these are tentative, and numerous other combinations of running periods are possible, depending on the physics landscape at the time. Not shown are **technology upgrades** to higher energies of 1 TeV and beyond. For these, a construction and installation phase of 3 years each is foreseen. The necessary R&D can be carried out in the shadow of running in scenario A or B.

3 Resource requirements

3.1 Construction cost and costing methodology

The capital cost of all stages in the scenarios A and B sketched above as well as the annual costs of operation are given in Table 1. No cost estimates are given here for later stages of the project for energies beyond 550 GeV.

The human resources requirements for the construction of the initial stage of scenario A amount to 10 120 FTEy, and to around 13 770 FTEy for scenario B (i.e. when starting at 550 GeV).

All cost estimates given here for scenario A or B stages are based on the ILC technical design report (TDR) [1] from 2012 and several cost updates performed since then:

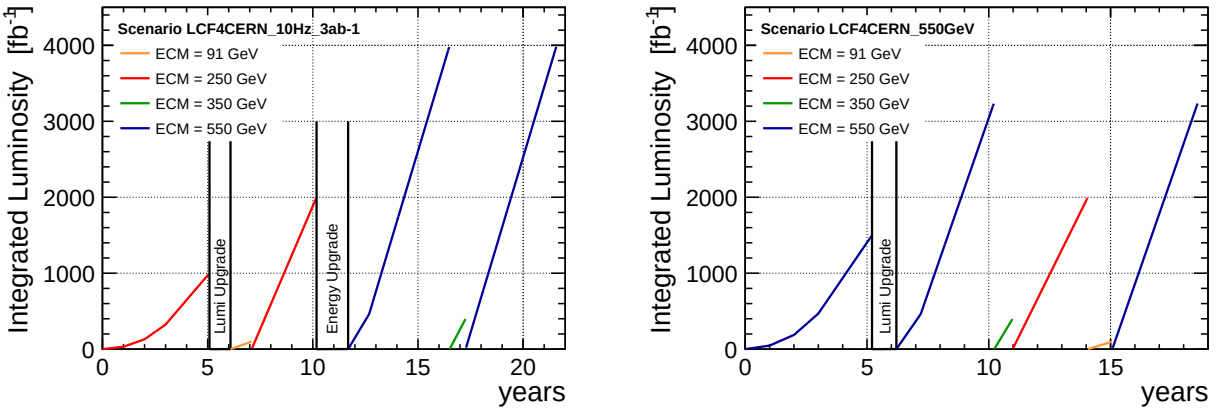

(a) (b)

Figure 4: Suggested run plans for an LCF at CERN (a) starting in the baseline configuration in scenario A, and (b) starting directly at 550 GeV. The technical time zero would be around 2044.

- the cost estimate for a staged 20.5 km, 250 GeV configuration of the ILC as a Higgs factory in Japan from 2017 [2], which was based on the cost basis of the TDR estimate from 2012, but included the effect of a reduced length and centre-of-mass energy as well as a number of minor design updates;
- the 2024 updated cost estimate of the ILC in Japan performed by the International Development Team (IDT) [3, 4];
- a new cost evaluation of the construction costs for the CERN site from 2025 [5].

The ILC cost estimate for the TDR [1] is a full bottom-up cost estimate based on around 2000 line items, going down to the level of the cost of individual components such as cavities, couplers, or magnets for key cost drivers. The costs were evaluated and aggregated by an international team of experts and reviewed by an independent international expert panel in 2013. The updated 2024 cost estimate was again reviewed by an international expert panel in Dec. 2024. A more detailed description of methodology, results and review are now contained in the addendum to the ILC submission to the EPPSU [3].

The scope of the cost estimate encompasses the construction cost for the accelerator systems as detailed in the TDR, with applicable design changes. Detectors are excluded, but detector assembly buildings, underground experimental halls, and detector access shafts are included. Computing equipment for accelerator operation is included, while computing installations for detector operation, data taking and analysis are excluded. The cost estimate covers the 10 year construction time until start of commissioning, and therefore excludes costs for project engineering and design, and for R&D prior to construction authorization, as well as costs for commissioning, pre-operation, operation, and de-commissioning. Taxes, contingency, and escalation during project construction are not included. Costs for upgrading the machine beyond 550 GeV are not included, except the cost of those systems that would be very difficult to provide after construction of the 550 GeV machine, in particular the main beam dumps and the beam delivery system (BDS). Costs for land acquisition and site activation (external roads, water supplies, power lines) are not included.

The scope of the new civil engineering cost estimate [5] encompasses the construction costs for underground buildings (tunnels, caverns, shafts) based on a design for the CERN site (Figs. 2 and 3), with tunnels and a central cavern for two beam delivery systems, adapted from the ILC TDR design to accommodate a possible later installation of CLIC. It also encompasses costs for accelerator-related surface buildings for cryogenics, cooling and power infrastructure, and for surface infrastructure in support of the detectors.

As discussed above, costs for land acquisition and site activation (external roads, water supplies, power lines) are **not included**, nor are costs for spoil removal.

The estimated amount of **spoil**, including a bulk factor of 1.3, is $2.7 \times 10^6\,\mathrm{m}^3$ ($1.9 \times 10^6\,\mathrm{m}^3$) for the 33.5 km (20.5 km) long facility. The corresponding costs are estimated to be 200 and 140 MCHF, respectively.

The methodology adopted for the ILC cost estimate was chosen as deemed appropriate for the ILC as an international, in-kind contribution project, with no specific site or host country identified at the time of the TDR. Civil infrastructure (separated in costs for construction and for infrastructure such as electric power supply, water systems, heating, ventilation and air conditioning (HVAC) and several other systems) was evaluated for three potential sites, one in Japan, one in the United States, and one at CERN. The costs were separated into "Labour" and "Value", where "Labour" corresponds to the total work performed by staff of participating institutions, measured in full-time equivalent person years (FTEy), while "Value" corresponds to the monetary value of goods and services procured from commercial vendors, expressed in ILCU2012 (ILC Currency Unit). An ILCU2012 corresponds to the purchasing power of 1 USD in the United States in Jan 2012. Comparisons between prices obtained in different countries were made on the basis of PPP (purchasing power parity) conversion rates, as evaluated and publicised by the OECD and World Bank. Where price information from several vendors was available, in particular for SCRF components, prices were converted to ILCU2012 and the lowest reasonable price (where "reasonable" takes into account whether the offering company has been demonstrated the capability to meet the required specifications) was adopted as price estimate. The information of the country of origin and currency of the original offer was retained, so that all quotations can be traced back to the original prices.

The **estimate for institutional Labour** of the 550 GeV configuration was taken from the TDR estimate [1] and amounts to 13.77 kFTEy, the estimate for the 250 GeV configuration is taken from the 2017 staging report [2] and amounts to 10.12 kFTEy.

For the 2024 IDT cost update [3], approximately 75 % of the costs were re-evaluated based on new quotations for SCRF components and updated civil engineering prices for the Japanese site. The costs that were not re-evaluated covered the more conventional accelerator systems such as magnets, vacuum system, diagnostics, etc. Those costs were converted back to the original currency, escalated with the respective region's inflation index for machinery and equipment, and converted to an updated ILCU2024, defined as purchasing power of a USD in January 2024 in the United States.

A cost estimate for the Linear Collider Facility at CERN was derived based on the described inputs, with a number of important differences:

- The Value estimate was converted to a procurement cost, expressed in 2024 Swiss Francs (CHF).
- The cost estimate was adjusted to take into account differences in the design of the facilities, such as different beam energies, the presence of a second BDS, and different RF configurations.

- The cost estimate for the construction costs of tunnels, caverns, shafts and surface buildings was based on a new study for the CERN site performed in early 2025.
- The cost estimate for the other civil engineering infrastructure (electric power, water, HVAC, etc.) was based on the costs evaluated in the 2012 TDR for the CERN site, escalated with the Swiss inflation index for machinery and equipment.

The conversion from Value to actual Cost in Swiss Francs takes into account a procurement model appropriate for a CERN-based project, different from the ILC approach to quantify the Value of goods: The ILC is a project based on international in-kind contributions, where the procurement is done separately by the contributing institutions, subject to price differences and possibly with a motivation to procure locally at potentially higher prices. This is a reason to consider the Value of contributed goods in lieu of the actual procurement cost in order to determine the monetary value of contributions to the overall project as laid out in a cost-book, which is not the same as the sum of all costs paid. In contrast, a CERN-based project would predominantly organise a central procurement on the world market, and consider the cost of purchased goods, converted to CHF based on market currency exchange rates.

To convert the ILC Value numbers to **Cost expressed in CHF**, all item values were converted from ILCU2024 back to the local currency (i.e. US Dollars, Japanese Yen, Euros, or Swiss Francs) and then converted to CHF with exchange rates as of January 2024. For goods that are available from different vendors around the world this is a conservative estimate insofar as the lowest reasonable price assumed in the ILC cost estimate is based on a PPP comparison, which leaves the possibility that the goods may be acquired in a different region of the world where price levels are lower than estimated from PPP rates.

The total cost for the baseline configuration LCF 250 LP amounts to 8.29 BCHF, for the full configuration LCF 550 FP to 14.53 BCHF in 2024 prices. These values are also summarised in Table 1, and they are broken down according to accelerator areas and to technical systems on the left and right side, respectively, of Fig. 5.

Design differences that were taken into account between the ILC design for Japan and the LCF design for CERN are:

- a second BDS: To account for the cost of a second BDS, all costs associated with the BDS and the interaction region were doubled, with the exception of the construction costs, because those were evaluated separately to include a design for the 2nd BDS;
- beam energy and main linac length;
- cryogenic power, arising from different repetition rate and different quality factor Q_0;
- CERN being not a greenfield site: The ILC cost estimate assumes a greenfield site and thus includes cost items that are already present at CERN, in particular investment for computing (computing centre and computing capacity for accelerator simulation and operation, without the computing capacity for the experiments). These items were removed from the cost estimate for CERN.

Some performance differences between ILC and LCF are considered to arise from successful R&D, with the assumption that these performance improvements will not affect component costs. These are in particular:

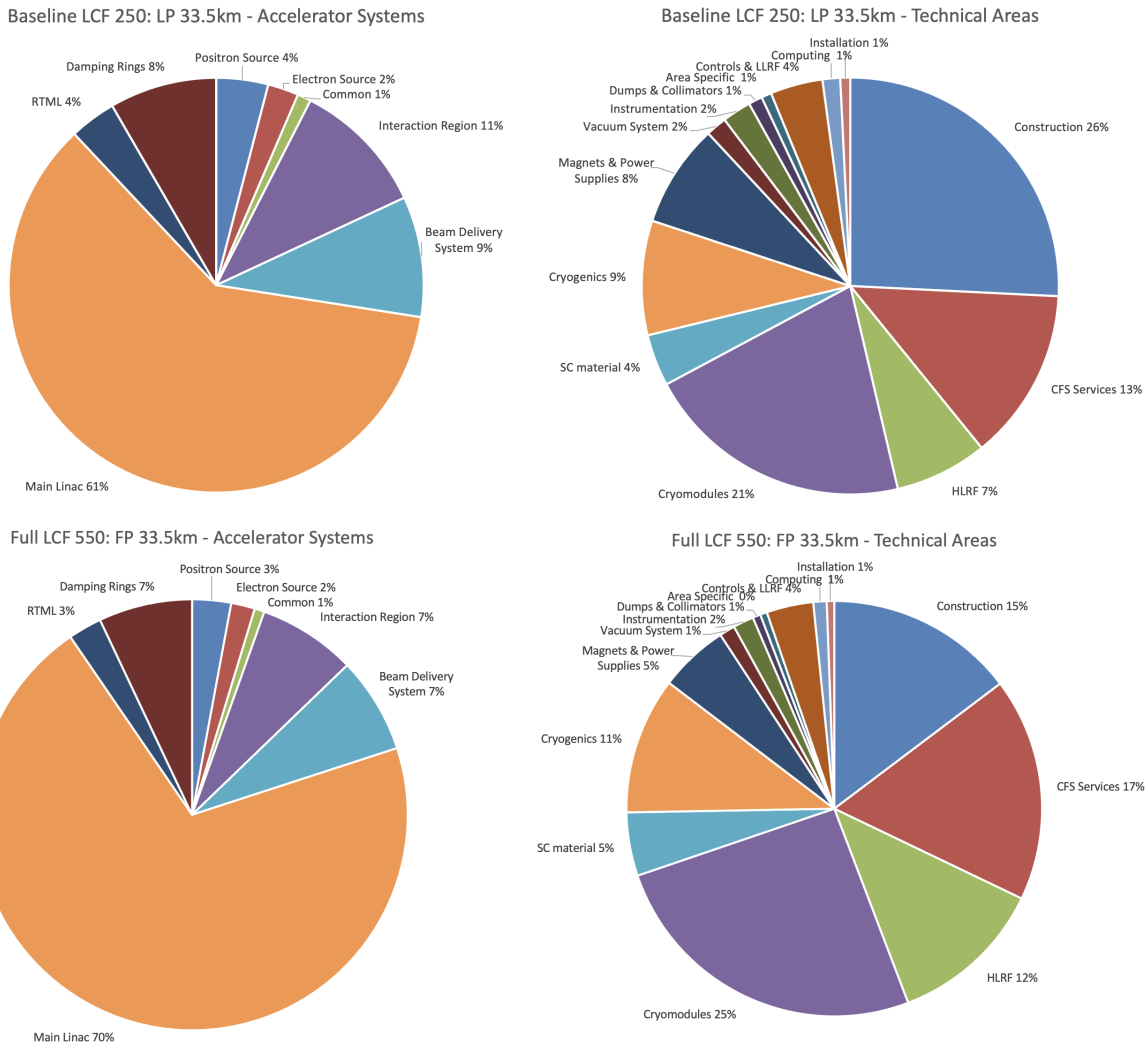

Figure 5: Costs for a Linear Collider Facility at CERN in the baseline 250 GeV low-power (1312 bunches) configuration (top) and the final 550 GeV full-power (2625 bunches) configuration (bottom), broken down according to accelerator areas (left) and technical systems (right). The total cost for the baseline configuration LCF 250 LP amounts to 8.29 BCHF, for the full configuration LCF 550 FP to 14.53 BCHF in 2024 prices.

- an increase of the quality factor Q_0 of the superconducting cavities from 1×10^{10} to 2×10^{10}: This increase is achieved by a modification of the heat treatment recipe, which is not expected to have a sizeable cost impact, assuming that the overall yield stays the same;

- better klystron efficiency, increased from 65 % to 80 %: This improvement results from a change in the electron optics of the klystron, based on a better design [6]. While this makes the klystron larger and heavier, the cost increase is hard to quantify and it is assumed that any resulting cost increase is covered by the cost uncertainty assigned to this item.

The cost uncertainty, or cost premium, of the cost estimate is defined as the difference between cost estimate at 50 % (median) and 84 % confidence level, which for normally distributed data corresponds to a 1 σ uncertainty.

The uncertainty associated with each cost element depends on the nature, quality and maturity of the basis of estimate for that element. In the TDR estimate, uncertainties were evaluated by cost estimators for each cost element, based on defined guidelines, taking into account:

- the maturity of the item's design (conceptual, preliminary, or detailed);
- the level of technical risk involved in the design and manufacture of the item;
- the impact of delays in this item on the project schedule (critical-path impact, non-critical-path impact, no schedule impact on any other item);
- the source of the cost information (engineering estimate based on minimal experience, engineering estimate based on extensive experience, vendor quote, industrial study, catalogue price);
- the extent, if any, of cost scaling to large quantities.

Uncertainties from the TDR were retained; for new estimates, uncertainties are determined according to the same guidelines.

For line items whose cost estimate has not been updated in 2024, but has been escalated from 2012 prices, the uncertainty of the regional escalation factor has been evaluated, and the resulting error has been added in quadrature to the original cost premium.

Cost premiums of line items are added linearly, which corresponds to treating all uncertainties as fully correlated and is a conservative approach[1].

The cost uncertainty reflects cost risk, i.e. uncertainties or errors in the cost basis (e.g. procurement of a similar item, quantity discount from a single unit price, engineering estimate, etc.) on which the cost of a specific item is based. This is to be distinguished from **technical risk** that is related to failure of a specific item to achieve the design performance, requiring a redesign which may result in schedule delays and increase the cost, and from **schedule risk** that is related to failure to supply a specific item on schedule, requiring delays which may increase the cost (typically by introducing inefficiencies and additional manpower requirements). **Market risk** is related to deviations in procurement costs from the estimate, due to changes in economic market conditions between when the estimate was made, and when the procurement is made. **Contingency** is a broader term, and includes not only cost uncertainties but also, for example, allowances for missing items. Performance risks and opportunities are discussed in detail in Sec. 8.
The resulting cost premium for the overall cost has been determined to be 29 %.

3.2 Operating costs

Operational year and energy consumption The assumptions on the operational year are summarised in Table 3. The numbers correspond to an availability of 75 %, in accordance with ILC design parameters. The approach follows the one laid out in [7] for FCC-ee and CLIC.

The power consumption, relative to the power for data taking, has been calculated under the following assumptions: Four operating modes are assumed – data taking, standby, shutdown, and machine development. In standby mode, RF is switched off, but all other systems are assumed to be operational. This saves between 46 % and 56 % of power. Standby mode is assumed to correspond to the state during down time and technical stops. In shutdown mode, RF is switched off permanently, so that the cryogenic load is reduced to about 32 % of its nominal value (calculated from the ratio of static to total cryogenic load, see [1, Tab. 3.11]) as well as magnets and other accelerator systems are switched off. Remaining power loads are the civil infrastructure (lighting,

[1] Treating them as uncorrelated would lead to an unrealistic reduction of the cost uncertainty when large cost items are split into smaller ones

cooling, ventilation, etc.), and cryo plants satisfying the static load. In this mode, between 25 % and 28 % of the nominal power are estimated to be consumed. These operating scenarios are the basis for the calculation of the total yearly energy consumption, as summarised in Table 5.

		Fraction of peak power			
Operational phase	days/year	LCF 250 LP	250 FP	550 LP	550 FP
Annual shutdown	120	28 %	18 %	28 %	25 %
Commissioning	30	77 %	72 %	75 %	72 %
Technical stops	10	54 %	45 %	50 %	44 %
Machine development	20	77 %	72 %	75 %	72 %
Downtime (faults)	46	54 %	45 %	50 %	44 %
Data taking	139	100 %	100 %	100 %	100 %

Table 3: Operational phase definition, with relative power consumption for each operation phase in relation to the nominal operating power assumed in the electricity consumption calculation.

Operating costs are summarised in Table 4. They were calculated taking into account the yearly electricity consumption, at a price of 80 CHF per MWh, and the costs for spares and maintenance.

Spare and maintenance costs were evaluated in relation to the construction costs as follows: Construction items are categorised into

- fixed accelerator installation, taken to be the total costs for cryomodules, magnets, vacuum system;
- consumables, taken to be the costs for all other accelerator components, i.e., HLRF equipment, magnet power supplies, dumps, and cryogenics[2], area-specific equipment such as source targets and guns, controls and LLRF, instrumentation, and computing;
- technical infrastructure, taken to be the costs for civil infrastructure such as water cooling, electric power infrastructure, air handling, installation equipment, and 10 % of the civil construction cost,

and assuming a replacement and maintenance cost per year of 1 % / 3 % / 5 %, respectively, of the corresponding capital expense. The operating costs for cryogenics includes the costs for liquid helium losses.

Human resource needs for operation have been estimated for the ILC [9] to be 850 FTE for the 500 GeV and 638 FTE for the 250 GeV machine. These numbers are consistent with estimates for CLIC [10] and the general experience at CERN.

4 Sustainability and environmental impact

The construction and operation of large-scale accelerator infrastructures such as the planned LCF at CERN require considerable resources and therefore entail a significant impact on the environment throughout the lifecycle of the project. As scientists and citizens, we acknowledge our obligation to future generations to plan our projects in the most sustainable way possible. Optimisation requires quantitative knowledge of the burdens imposed by the construction, operation and demolition of the

[2] For cryogenics, experience from LHC indicates that the yearly operating and maintenance costs are 2.8 % of the original invest, which includes the costs for replenishing liquid helium losses [8].

Operating costs	LCF	250 LP	250 FP	550 LP	550 FP
Nominal operating power	MW	143	182	250	322
Yearly electricity consumption	TWh	0.8	1.0	1.4	1.8
Electricity price	CHF/MWh			80	
Yearly electricity costs	MCHF	66	77	115	142
Fixed accelerator inst. (1 %)	BCHF	2.8	2.9	5.2	5.3
Consumables (3 %)	BCHF	2.4	2.8	4.0	4.8
Technical infrastructure (5 %)	BCHF	1.1	1.4	2.0	2.5
Operation & maintenance	MCHF/y	156	182	273	322
Total yearly operation costs	MCHF/y	222	259	388	464
Personnel	FTE	640	640	850	850

Table 4: Operating costs, for electricity and operation and maintenance (including helium, see text).

entire facility. To this end, the ILC and CLIC projects have commissioned two lifecycle assessment (LCA) studies with ARUP, a consultancy company [11, 12]. These lifecycle assessments form the basis for the greenhouse gas (GHG) emission numbers summarised in Table 5.

A first study [11] quantified the environmental impact of the civil construction of the underground tunnels, caverns and shafts of the ILC and CLIC in several configurations, as it was assumed that this would constitute the largest contribution to the overall emissions. The study was based on the detailed available designs of the underground installations and considered the relevant construction methods. In particular the tunnelling methods chosen are different: the ILC in Japan will use the New Austrian Tunnelling Method (NATM), a drill–and–blast method, in a solid granite geology, while at CERN a tunnel boring machine would be used in molasse rock. The resulting tunnel cross sections differ substantially in shape and in the amounts of material used for grouting, lining, rock bolts, and reinforcement steel. This is reflected in the LCA. The numbers quoted for the LCF at CERN are based on these analyses, which is possible as the LCF's tunnel design closely follows the CLIC design.

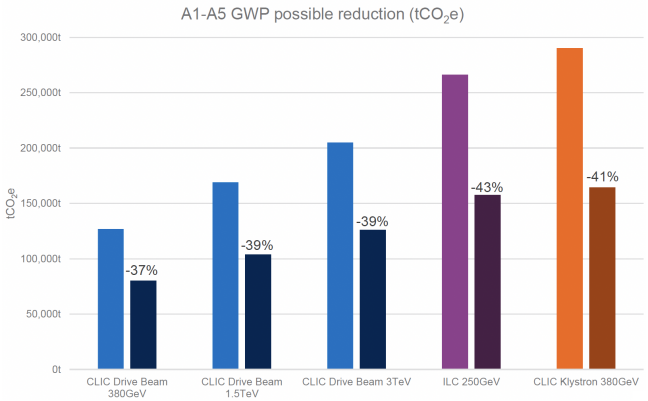

Figure 6: CO_2 emission reduction opportunities for the ILC and CLIC underground facilities identified in an LCA study of underground civil construction [11].

The purpose of this and other life cycle assessment studies is not so much to produce a set of numbers that quantify the environmental impact, in particular the global warming potential (GWP) as a measure of effective greenhouse gas emissions, as to provide quantitative data early in the project to reduce the impact as far as possible. Important conclusions that can be drawn from the LCA study of underground facilities are:

- Given the low carbon intensity of French electricity, for a project at CERN the embodied carbon in civil construction by far surpasses that arising from electricity consumption.
- The GHG impact of underground structures is by far dominated by the embodied carbon in the materials used for construction, in particular cement (around 85 %) and steel (around 15 %).
- The GHG impact of concrete and steel can be substantially (more than 40 %) reduced by optimising the design (e.g. by a reduced lining thickness) and by usage of carbon-reduced materials, in particular as cement[3]. The overall reduction opportunities are shown in Fig. 6.

A second, more comprehensive study [12] also quantified the environmental impact of the accelerator and detector construction for the CLIC and ILC designs. Owing to the enormous complexity of an entire particle accelerator and the detectors, with a multitude of different components and materials, an LCA of a complete accelerator project is extremely challenging. Nonetheless, an attempt was made to quantify the overall impact by focussing on the most abundant and material-intensive systems and components, in particular the magnets and accelerating RF structures. Because some materials, in particular very pure niobium used in superconducting cavities, are specific to accelerators, so that no lifecycle data have been available in the usual databases, detailed studies of these materials were necessary as part of the overall effort. The same applies to specific production methods such as electropolishing used in the cavity fabrication. This study also made an attempt, for the first time, to quantify the environmental impact of the operation phase beyond the electricity consumption (e.g. the impact of spare part production) and of the demolition stage with the recycling or disposal of materials.

Some important conclusions from this study:

- The GHG impact of the accelerator and detector installations together is as big as or even bigger than the impact of civil construction.
- The impact is dominated by the embodied carbon in the materials used; material processing (e.g. refinement by electron beam melting) for specific material qualities required for accelerators (ultra pure niobium, oxygen free copper) plays an important role and cannot be neglected in the analysis.
- Again, significant reduction opportunities exist, but owing to the multitude of components and materials these are more diverse than in the civil construction case and require careful individual assessment.
- The GHG impact of electricity consumption depends on the location of the project and on the time of (first) operation owing to envisaged carbon reduction measures in the electricity sector. Assumptions about these parameters have ramifications for the overall system optimisation (embodied carbon versus operation).
- Detectors contribute a sizeable amount to the GWP impact, dominated by the iron required for the magnet return yokes.

The data gathered in this study were also used to estimate the CO_2 impact of an LCF at CERN, based on ILC technology, as summarised in table 5. The ILC data were adjusted, to the extent possible, for design differences, in particular a second BDS, a third damping ring for full power (2625 bunches) operation, longer tunnel lengths, and different centre-of-mass energies, to estimate the LCF numbers.

[3] For instance, usage of cement with 50 % addition of GGBS (ground granulated blast-furnace slag) would provide a 22 % overall CO_2 reduction.

	ILC 250	ILC 500	LCF 250 LP / FP	LCF 550 LP / FP
CoM energy [GeV]	250	500	250	550
Luminosity/IP [10^{34} cm^{-2}s^{-1}]	1.35 / 2.7	3.6	2.7 / 5.4	3.85 / 7.7
Number of IPs	1		2	
Operation time for physics/yr [10^7 *s*/*yr*]	1.6		1.2	
Integrated luminosity/ yr [1/fb/ yr]	215 / 430	580	325 / 650	460 / 920
Host countries	Japan		France and Switzerland	
GHG emissions from construction, stages A1-A5				
Subsurface tunnels, caverns, shafts [kt CO_2e]	266	372	380	
Accelerator (coll.) [kt CO_2e]	150	270	165	310
Accelerator (inj.) [kt CO_2e]	59 / 82	83	60 / 84	
Services [ktCO_2e]	32	46	46	
Detectors [kt CO_2e]	94		94	
Total [kt CO_2e]	601 / 624	865	745 / 769	890 / 914
Collider tunnel length [km]	20.5	33.5	33.5	
Collider tunnel diameter [m]	9.5		5.6	
Collider tunnel GHG / m [t CO_2e/ m]	8.6		8.5	
Concrete GHG [kg CO_2e/ kg] / [kg CO_2e/ m^3]	0.16 / 400 (C25/30)		0.16 / 400 (C25/30)	
Main Linac accelerator GHG / m [t CO_2e/ m]	5.3		5.3	
GHG emissions from operation				
Maximum power in operation [MW]	111 / 138	164	143 / 182	250 / 322
Annual electricity consumption [TWh/ yr]	0.7 / 0.9	1.1	0.8 / 1.0	1.4 / 1.8
Reference year of operation	2040		2050	
Carbon intensity of electricity [g CO_2e/ kWh]	81		16	
Average Scope 2 emissions / yr [kt CO_2e]	59 / 74	87	13 / 15	23 / 28

Table 5: Data on GHG emissions for the ILC project in Japan and the Linear Collider Facility proposal for CERN. These are baseline numbers, before application of possible CO_2 reduction measures. The optimisation potential for tunnels, caverns and shafts is estimated to be 50 %, for accelerators, services and detectors it is assumed to be 25 %.

The peak and annually integrated energy consumption during each stage of operation is given in Table 5, together with the integrated carbon-equivalent energy costs for the construction of the various stages. The required site AC power ranges between 143 MW and and 322 MW for the initial 250 GeV and the final 550 GeV machine.

Further environmental impacts are expected to be small in comparison. In particular it is assumed that direct emissions from detectors of green house gases with very high weighting factors such as chlorofluorocarbons (CFC) or SF_6, which currently dominate CERN's GHG emissions [13], will be fully curtailed in a future project by adequate protection measures. As additional information, Table 6 gives the estimated land use of the LCF project at CERN. It includes both CERN attributed fenced land ("fenced") and CERN attributed unfenced land ("unfenced"). CERN buildings and infrastructure include constructions and installations, both above and below ground. The third category is land outside the attributed areas ("outside"). For the LCF it is possible to move the IP surface infrastructure partly or fully inside the "fenced" area if this is advantageous. Re-use of fenced land is not considered "consumed" in this summary.

5 Technology and delivery

In principle, all **key technologies** for the 250 and 550 GeV machines **are mature and construction-ready**. In particular, the superconducting radio-frequency technology is extremely well understood and at the heart of well-established and excellently performing machines like the European XFEL in

	20.5 km machine	33.5 km machine
Number of new access shafts (outside/unfenced/total)	4 / 3 / 7	8 / 3 / 11
Number of new surface sites (outside/unfenced/total)	4 / 1 / 5	8 / 1 / 9
Area of land permanently consumed (outside/unfenced/total) [km^2]	0.12 / 0.13 / 0.25	0.21 / 0.13 / 0.34
Area of surface constructions (outside/unfenced/total) [km^2]	0.022 / 0.033 / 0.055	0.040 / 0.033 / 0.073

Table 6: Area of land occupied by the LCF project at CERN.

Hamburg, Germany, or the LCLS II at SLAC, USA. Still, compared to e.g. the ILC TDR from 2013 [1], significant R&D progress has been achieved in terms of, e.g., gradients, quality factors (Q_0), energy efficiencies, and repetition rates (see Sec. 3.1 "Some performance differences"). A discussion of the R&D progress and European XFEL operation experience on which the LCF capitalizes can be found in [14].

The overall technological readiness of the project is reflected in the timeline discussed in Sec. 2 and shown in Table 2. The necessary steps are given separately for the preparatory phases 1 and 2 defined in the main document of this submission. The following subsections 5.1 and 5.2 discuss the most important remaining R&D topics and necessary technology choices and the TRL levels of individual sub-systems of the machine, respectively.

5.1 Overview, R&D requirements and next steps

Despite the overall technological readiness of the project, some R&D needs to be carried for certain aspects of an LCF machine, and important studies for siting etc. are required, each with significant durations. The work is split up into two preparation phases of three and five years, respectively, see Tab. 2. The most time-critical aspect is the exact siting – i.e. a detailed placement study, which might even be technology-independent. Furthermore, also definite parameter choices (e.g. gradient versus number of cryomodules) need to be made. Both will be addressed in Phase 1, while Phase 2 will lead up to a full CFS planning and an engineering design.

Note that the start of the second phase – here assumed at a time T_0 – would require a formal decision to proceed with the project. Likewise, the construction start at T_1 requires a formal decision by CERN Council. Note further that in Tab. 2 the construction time is increased beyond the purely technical limitation of eight years to ten years in order to accommodate the fact that the transition between phases might require some time, and also to avoid the clear conflict between HL-LHC operation and beam commissioning of a new collider.

Phase 1, ideally starting directly in 2026 after the finalisation of the EPPSU, builds on and integrates the on-going work of the ILC Technology Network (ITN) on the key technologies [3, 15], complementing it with siting and implementation studies, in parallel with design and technical studies to determine and confirm the final LCF parameters. This phase is required to prepare a project decision by CERN Council, which is not expected before 2028, and should deliver:

- **Final placement of the collider complex** and its infrastructure after assessment of their territorial compatibility, both for its initial phase and potential upgrades. Preparation and documentation for wider implementation studies with the host regions / states in Phase 2.
- **Optimisation of LCF design:** Review of the accelerator design along with updated cost, power and risk assessments, including in particular:
  - a detailed design of the Interaction Region for two experiments – including re-optimised Beam Delivery Systems – that is suitable for an initial SCRF-based accelerator as well as for future technology upgrades like CLIC, C^3, ERLs or PWA;

  - studies of the implications for Civil Engineering and the equipment used in the initial SCRF based facility, in order to allow collider upgrades in the future, and to accommodate the "beyond colliders" physics programme described in the main document;
  - design and parameter optimisation of the entire machine including further nanobeam studies. This comprises an R&D programme to develop prototypes of key components with regard to performance and cost risks and opportunities, or with ramifications for the CFS design, in particular cavities, cryomodules, klystrons, RF input couplers, main dumps, and the positron source target and capture device.

The estimated resources needed for Phase 1 are 35 MCHF material and 180 FTEy of personnel effort. These resources are backed up by the ITN efforts that, over 5 years, amount to around 30 MCHF and about 250 FTEy.

Phase 2 would require a decision to go ahead with the project preparation as needed to start construction. It targets the final engineering design, larger industrial pre-series and an extensive site preparation, in particular:

- SCRF industrialisation of a design based on more ambitious goals for cavity quality factors (Q_0) and power (klystron) efficiency, with higher repetition rate and hence cryogenic needs than foreseen in the ILC TDR design. This task builds on the work of the ITN [15];
- detailed studies of the Cryogenics system and Infrastructure Systems (e.g. cooling and ventilation, electrical, access and safety systems, transport and installation) adapting them to standard solutions used by CERN and industry;
- final site preparation including documentation and specifications for the time-critical civil engineering contracts.
- environmental studies and integration of the collider in the local area with the host states.

The estimated resource needs for Phase 2 are 120 MCHF for pre-series and 420 FTEy of personnel effort for the technical studies, pre-series, engineering design and laboratory infrastructure. With the widespread expertise built up worldwide for SCRF based free-electron lasers (e.g. the European XFEL or LCLS-II) as well as for the ILC, a significant part of this work can be done outside CERN for an LCF starting with SCRF technology. In parallel, civil engineering preparation including continued environmental studies will require significant resources, typically 5% of the civil engineering budget.

Also during the preparation period, detector collaborations need to be prepared and set up, building on the experience of the numerous detector concepts for Higgs factories, but also embracing new ideas.

5.2 Assessment of technology readiness

The technological readiness of the ILC has been scrutinised by the Implementation Task Force in the context of the Snowmass process in 2021 [16], with the result that all areas considered were given the highest mark, corresponding to a Technology Readiness Level (TRL) of 7 to 8, except the positron source, which was assigned the second highest category, corresponding to TRL of 5 to 6. Parallel to that, the IDT formulated a plan for a preparatory lab [17], identifying the most important R&D topics, based on considerations of technical risk, but also cost risks and opportunities. Based

on a revised version of this plan [15], the International Technology Network (ITN) has been formed that now actively pursues these issues.

In the following, we discuss the most important R&D topics and give our own assessment of technology readiness. We follow the TRL definitions given in [16, Appendix A.7], which are closely aligned with the definitions in the DOE Technology Readiness Assessment Guide [18].

Cryomodules and cavities Cryomodules with a design that is almost identical to the design foreseen for the LCF have been successfully produced in series for the European XFEL, and very similar ones for LCLS-II, and have been in operation at the European XFEL since more than 8 years without problems. Industrial production of cavities with more than 800 cavities produced for the European XFEL alone has been demonstrated [19, 20], with many cavities surpassing ILC specifications. For ILC specifications, the remaining risk is not any more of technological nature, but predominantly concerning the production yield. The resulting cost risk is small, as a 90 % production yield is already factored into the cost calculation, and a further yield reduction of e.g. 10 % would lead to only a few percent overall project cost increase.

The operating gradient of 31.5 MV/m required for the LCF has also been demonstrated for complete cryomodules [21]. All key components (couplers, cavities, tuners, cold mass and vessel) have been successfully produced in industry (**TRL 9**). The main parameter to be improved is the quality factor Q_0 at the operational gradient of 31.5 MV/m, since the LCF assumes improved performance in cavity quality factor ($Q_0 = 2 \times 10^{10}$ instead of 1×10^{10}) at an average operational gradient of 31.5 MV/m. Successful industrial series production of cavities with these performance parameters has to be demonstrated; with regard to the quality factor, we rate the cavities **TRL 7** (prototype demonstration in operational environment).

Overall, superconducting TESLA-type cavities and cryomodules for the main linac have been fully industrialised and thus do not constitute a technological risk for the construction of a superconducting linear collider facility as proposed, which is a main strength of the proposal. As cavity and cryomodule production (including costs for superconducting material) constitutes 25 % of the overall cost of the proposed LCF, successful R&D offers large benefits in terms of performance and construction cost, which is why this is considered a high priority item. For a more in-depth discussion of the risks and opportunities related to cryomodule performance see Sec. 8.

The time-critical work packages WP'1 (cavity production) and WP'2 (cryomodule assembly) of the ITN [15] have been created to conduct this R&D. In the context of a preparatory study for an LCF at CERN, these activities should be further intensified.

Positron source The baseline source design for the ILC as well as the LCF is the helical undulator positron source, which provides polarised positrons at a rotating target from polarised photons created in a helical undulator operated with the accelerated electron beam. The basic principle (production of polarised positrons from photons generated in a helical undulator) has been demonstrated in a successful experiment (E166) at SLAC [22, 23].

The status of the ILC positron source has been summarised by the positron working group [24]. Since then, significant progress has been made on several fronts [25, 26]. This system has a number of critical key components:

The superconducting helical undulator comprises a number of modules that form a 230 m long undulator section, creating a highly collimated, narrow beam of photons. Helical undulators have been successfully produced, a prototype design for a cryostat as required for the ILC has been successfully built and tested [27]. The operation of long undulator sections in high-energy beams is state of the art, e.g. at LCLS, PAL-XFEL and European XFEL [28–30]. A fully operational undulator module with the required parameters (k-value) would be the next step.

The design of the positron production target foresees a rotating wheel made of titanium alloy, cooled either by radiation or heat conduction via friction [31]. The engineering challenges are vacuum tightness of the rotating assembly, sufficient cooling and damage from shock waves created by the pulsating photon beam. Due to the large activation of the materials, a remotely operated target exchange mechanism is required. First engineering prototypes of a rotating target have been built. Target materials have been characterised in test beams, demonstrating the required radiation hardness [32]. Overall, we consider the target design **TRL 5** (component validation), consistent with the evaluation of the ITF. A next step will entail a fully operational target, operating at the required parameters (vacuum, rotational speed, cooling, operation in presence of pulsating magnetic field of capture device), which would raise the TRL to 6.

For the positron capturing device, several design ideas exist. The most promising design is based on a pulsed solenoid design [25]. Pulsed solenoids have been successfully operated in other accelerator applications. An engineering study of a pulsed solenoid is under way. We consider the pulsed solenoid **TRL 5** (component validation). A next step entailing a fully operational pulsed solenoid – operating at the required parameters (field strength, pulse shape, flat top length, aperture) – is underway in the context of the ITN. This would raise the TRL to 6.

The photon dump, in particular its entrance window, is also challenging owing to the fact that changing the entrance point by moving the beam spot ("painting") is not possible.

The work packages WP'6 (rotating target), WP'7 (magnetic focusing system) and WP'11 (target maintenance) of the ITN [15] have been created to conduct the time-critical R&D aspects.

In the context of a preparatory study for an LCF at CERN, these activities should be further intensified.

As a risk mitigation strategy, an alternative positron source concept based on a separate electron beam impinging on a slowly rotating target (electron-driven source) has been developed over the last decade [33, 34]. Such a source concept has important advantages in terms of ease of operation, as it decouples positron production from the electron main linac; however, it does not provide positron polarisation. Should an undulator-driven, polarised positron source turn out to be too risky, a decision to build an electron-driven source would ensure that the project can proceed, albeit without positron polarisation. The time-critical work packages WP'8 (rotating target), WP'9 (magnetic focusing system) and WP'10 (capture cavity and linac) of the ITN [15] have been created to conduct further R&D on this concept.

Electron source photo injector gun High voltage photo guns with the characteristics required for the LCF have been built and successfully operated in accelerators, thus this system does not pose a technological risk. In order to take advantage of experience accumulated over the last decade, and to preserve the existing know-how, the time-critical work packages WP'4 (higher voltage ILC photo-gun R&D) of the ITN [15] has been created to continue these activities.

IP spot size / stability Focussing the beams to the required nanometre size and bringing them to stable collision is the core challenge of the nanobeam technology that makes any linear collider possible. This has been the topic of extensive R&D over the last decades, with dedicated test facilities where the necessary technologies can be tested and verified. The Accelerator Test Facility ATF2 [35, 36] is the main workhorse for this R&D. At ATF2, the final focus concept of the ILC, based on local chromatic correction, has been verified [37], together with the necessary beam stabilisation with the FONT feedback system [38, 39]. Based on the extensive testing at the ATF2, we rate the issue of IP spot size and stability to be **TRL 6** (technology demonstration in a relevant environment).

The time-critical work packages WP'15 (final focus) and WP'16 (final doublet) of the ITN [15] have been created to conduct further R&D.

Crab cavity A number of competing designs for the crab cavities around the interaction point have been put forward and assessed in a dedicated workshop [40], with a down-select of the two most promising designs for further R&D.

The time-critical work packages WP'3 (crab cavity) has been created to conduct the necessary R&D.

Damping rings The ILC damping ring design is similar to planned and existing storage rings for synchrotron radiation production. Key parameters are the same as those of operating facilities: with a 3.2 km circumference at 5 GeV beam energy, it is similar to PETRA III, and the normalised emittance $\gamma\varepsilon_{x/y} = 4\,\mu$m/20 nm has been achieved in operating light sources. Important challenges are the 400/800 mA beam current for electrons/positrons, which were tested at the CESR-TA test facility [41], the large dynamical aperture required for positron injection, and the small transverse (longitudinal) damping time of 13 (7) ms, to be provided by radiation damping from superconducting undulators. Lattices that fulfil the design requirements have been developed. Overall, we consider the damping ring system design to be **TRL 7** (prototype demonstration in operational environment), in agreement with the assessment by the ITF.

Further R&D concerning the overall damping ring system design is being conducted as ITN time-critical work package WP'12 [15].

Injection and extraction kickers Injection into and extraction from the damping rings requires kickers that are capable of kicking individual bunches at a minimal bunch separation of 3.2 ns. The damping ring bunch pattern consists of mini trains of about 25 consecutive bunches, followed by a gap of about 10 empty bunches. Bunches are extracted from the tail of these mini trains, therefore the rise time is the bigger concern. A prototype kicker has been tested successfully at ATF2 [42]. Therefore, we rate the kicker system to be **TRL 7** (prototype demonstration in operational environment), in agreement with the assessment by the ITF.

Further R&D into the design of the kickers is being conducted as ITN time-critical work package WP'14 [15].

Emittance preservation Preserving the very small emittance of the beam exiting the damping rings along the low energy (5 GeV) transport line [43, 44], the bunch compressors [45] and the main linac [46, 47] is a central element to achieving the required small beam spot sizes and thus the target luminosity, and has been extensively studied. An intrinsic advantage for emittance preservation are the large apertures of the accelerating L-band cavities, which lead to modest wakefield effects compared to accelerators operating at higher frequencies.

Therefore, we rate the emittance preservation to be **TRL 8** (system completed and qualified through test and demonstration), in agreement with the assessment by the ITF.

Main dump The ILC main dump is designed for up to 17 MW of beam power (for a single beam, sufficient for the 1 TeV upgrade of ILC), which is more than sufficient for the full LCF 550 configuration, where the maximum 23 MW beam power would be shared by two beam delivery systems and main dumps. The main dump design is based on a water dump, which follows the design of the SLAC 2 MW water beam dump that has been successfully operated in the past. An engineering design is required for a detailed planning of the enclosing cavern, including cooling, ventilation and treatment of generated isotopes, in particular tritium. The entry window of the dump is another important challenge.

The design of main dump, including prototyping of the entry window, is the topic of the ITN time-critical work package WP'17 [15].

Based on the fact that at SLAC a water dump was build and operated successfully, albeit at a lower power rating, we consider the main dump technological readiness to be **TRL 5** (component validation).

RF systems The RF systems (modulators, klystrons, power distribution system) required to operate the accelerator have parameters that are mostly identical to those of the corresponding systems of operational accelerators, in particular the European XFEL.

Klystrons with the required parameters (pulse length and output power) are commercially available and are in use in comparable facilities (TRL 9). The LCF proposal assumes that the efficiency can be raised from 65 % (commercially available) to 80 %, based on a design study for 1.3 GHz and experience from similar developments [6]. Because no prototypes for the specific operation parameters (1.3 GHz, 10 MW, 1.65 ms) have been built, we rate this as **TRL 4** (validated in laboratory environment). It is worthwhile to note that the klystron efficiency does not pose a technical risk to the LCF. If the expected efficiency improvement would fail to fully materialise, this would be know early enough to install more powerful modulators[4] and cooling systems. The resulting impact on construction and operation costs is in the few percent range.

A prototype of a design suitable for installation and operation in the accelerator tunnel with the required availability parameters would be beneficial. The modulator foreseen for the ILC (semiconductor-based Marx modulator design) is different from the modulator employed in the European XFEL (bouncer modulator and pulse transformer), operating at the full high voltage of the klystron without the need for a transformer. Prototype Marx modulators exist and have been tested, and we consider this **TRL 7** (prototype demonstration in operational environment), in agreement with the assessment by the ITF.

The waveguide power distribution system, although different in design from the European XFEL one, is comprised of commercially available components, i.e. **TRL 9** (proven through successful operations).

The main parameter to be improved is the klystron efficiency (65 % to 80 %).

HOM detuning / damping Absorption of higher order modes in SRF cavities of TESLA design uses the same design employed at the European XFEL. The components are commercially available from industry, the design has been proven at the European XFEL. We rate this topic to be **TRL 9** (proven through successful operations).

Component/Sub-system	TRL	Main parameter to be improved	Improvement factor	RF effort		
				Personnel [FTEy]	Material [MCHF]	Timescale [years]
Positron source	5	Target cooling Pulsed solenoid peak field	N/A	15	5	3
Main dump	5	Maximum power	8	N/A	N/A	N/A
IP spot size/stability	6	Vert. beam size at nom. bunch population	10 %	18	4	6
RF power sources	6	efficiency	1.2	10	3	3
1.3 GHz RF cavities/cryomodules	7	Q_0	2	30	10	3
Damping rings	7	Beam dynamics	N/A	10	3	3

Table 7: Technical readiness and R&D requirements for LCF@CERN.

All further stages, i.e. going to 1 TeV or beyond, require significant R&D. However, since these stages will enter any construction phase at the earliest in the middle of the 2050s, no critical paths or R&D needs can be discussed here in a meaningful way.

[4] Cost savings from reduced modulator capacity are not taken into account in the LCF cost estimate, which assumes 65 % in the costing, thus an 80 % is a cost reduction opportunity.

6 Dependencies

The described scenarios assume **CERN as a host site** for the Linear Collider Facility. However, the construction of an ILC-like machine has also been studied, naturally, for Japan, and other locations.

With its modest power needs and operation costs compared to other projects, the Linear Collider Facility in the stages up to 550 GeV centre-of-mass energy would not interfere negatively with other activities on the CERN site. In particular, a **rich scientific diversity programme** and a broad portfolio of advanced accelerator R&D activities (e.g. magnet developments, plasma, ...) could be maintained as an important complement to CERN's portfolio, as postulated also by the 2020 European strategy update.

The LCF realisation and operation at CERN does, in particular, not depend on the LHC injector chain and could thus be developed independently of the ongoing (HL-)LHC programme.

Furthermore, the realisation of the LCF programme at CERN does not entail the premature definition of the precise technology for a future 10 TeV parton-parton centre-of-mass energy collider.

7 Commentary on current project status

The ILC project has, since decades, assembled a **large community** supporting it and bringing it to the level of maturity that is observed today. This is also documented in the project TDR [48, 49], in the ILC staging report from 2017 [2], and e.g. in the report to the Snowmass process 2021 [50]. The ILC has been, in fact a **global project** for 20 years, with accompanying technology collaborations like the TESLA Technology Collaboration, TTC, for the advancement of SRF technology.

The **size of the community** of scientists who directly work on the project can be estimated from the number of institutions supporting the TDR (rougly 400) or the number of individuals that signed the Snowmass report (rougly 500). The relevant community event – the International Linear Collider Workshops (LCWS) – typically attract between 300 and 800 participants.

Another measure for the potential size of potential community is the expected **number of collaborators** for a facility with two large collider experiments and an ample and diverse "beyond colliders" programme attached. Assuming the typical size of an experimental collaboration of 3,000 members, and 1,000 members for the diversity programme, the Linear Collider Facility might be foreseen to hold a community of around 7,000 members. This leaves room for significant activities on continued HL-LHC data analysis, small and medium size experiments at CERN and national labs as well as intensified R&D towards the exploration of the 10-TeV scale and beyond.

The project in both scenarios A and B lends itself easily to the realisation of significant **in-kind contributions**. In particular the mass production of cryomodules – as already exercised in an industrialised fashion e.g. for the European XFEL – allows for distributed the production of attractive technology in different world regions. Several cavity vendors take a keen interest in the project, and the highly modularised production possibilities allow for a high added economic value.

8 Performance Risks and Opportunities

In this section, we discuss the most prominent risks and opportunities, mitigation strategies and possible impacts on cost, schedule and performance. We highlight risks and opportunities associated with superconducting RF technology, which have the potential to have the largest cost impact owing to the large cost fraction of the main linac SCRF components.

8.1 Accelerating gradient and collision energy

The operating gradient of the main linac cryomodules is directly linked to the achievable beam energy and thus the physics performance. For a Higgs factory with 250 GeV design energy, operation at an energy reduced by 8 % to 230 GeV would not compromise physics performance too much (e.g. ZH cross-section reduced by about 15 %) and thus would be acceptable initially. An undulator-based positron source, however, the yield falls off steeply at decreased electron beam energy, which raises the importance of achieving 95 % or more of the design energy at least for the electron beam from the start of operation. Thus in this section, we discuss risks and opportunities associated with the operating cavity gradient.

The baseline design of the ILC and the LCF assumes an average cavity gradient of 35 MV/m with a 20 % spread for cavities measured individually in a vertical test stand prior to integration in the cyro module, and a 31.5 MV/m average gradient for operation with beam. These are the same values as assumed in the ILC TDR. Experience from series production of cavities and cryomodules, in particular for the European XFEL (Eu.XFEL), and the ensuing operating experience, corroborate these values, and point to remaining challenges and opportunities.

Single cavity performance in vertical tests: The gradient performance of single cavities as received from vendors depends critically on the production and surface treatment process, and a rigorous quality control. The Eu.XFEL production model was build-to-print, where the vendor guarantees to follow the agreed production process rigorously, but is not required to assert a specific gradient. This model requires a close quality monitoring between vendor and customer during production, and permits a substantial cost benefit due to the reduced risk the vendor has to carry. Over all, 800 cavities were procured for the Eu.XFEL from two separate vendors, one of those (RI) applied the same surface treatment protocol as foreseen for the ILC, so that the performance of the cavities from this vendor provides an excellent sample for the expected performance of industrial cavity production, despite the fact that Eu.XFEL design gradient at 23.6 MV/m was substantially lower than the ILC design gradient. The performance of a cavity depends critically on surface quality and can be severely deteriorated by small defects, which can often be removed by a second or possibly third surface treatment, which can be a full chemical treatment (electropolishing) at the vendor, or a much simpler and cheaper high-pressure water rinse in the testing institution. Therefore, the protocol for acceptance or re-treatment of cavities has a decisive impact on the performance of the finally accepted sample, which needs to be taken into account when interpreting the Eu.XFEL results and calculating the expected performance resulting from the acceptance criteria for ILC, which ask for at least 28 MV/m in vertical tests. The results for the cavity production have been published [19, 51]: for the company (RI) that followed the ILC surface treatment recipe, the maximum gradient (gradient limited by quench or excessive field emission indicated by X-ray emissions) for cavities as received from the vendor was 33.0 MV/m, with a RMS spread of 6.5 MV/m (20 %), already very close to the ILC specification. The "usable" gradient, which requires in addition that Q_0 is better than the design value of 1×10^{10}, was 29.0 MV/m, with a RMS spread of 7.9 MV/m (27 %). Cavities were typically re-treated up to two times (mostly by high pressure water rinse) if the gradient was below 20.0 MV/m; for these cavities, high pressure rinsing typically improved the gradient by 8 MV/m.

After following the Eu.XFEL retreatment protocols, the average maximum / usable gradient of cavities from RI was 34.6 / 31.2 MV/m, averaged over both vendors the average usable gradient was 29.9 MV/m with a 5.2 MV/m (17 %) spread.

Cavities with gradients above the XFEL acceptance limit of 20 MV/m, but below the ILC limit of 28 MV/m were not retreated. An simulation of the effect of such a re-treatment regime [14, 20] concluded that with up to two re-treatments, the ILC gradient goal (35 MV/m on average, at least 28 MV/m) would be achieved for the usable gradient with a yield of 91 %, fulfilling the 90 % yield as-

sumption of the TDR that underlies the cost estimate. Thus, the Eu.XFEL production data fully validates the performance requirements for cavities after the vertical tests assumed in the ILC design, for an ILC specificatiom of $Q_0 > 1 \times 10^{10}$. The implications of the larger Q_0 requirement for the LCF will be discussed in the next section.

Performance in cryomodule at the test stand: During the Eu.XFEL production, cavity performance was measured again after installation in cryomodules for 100 % of the modules [52]. The results differ from the vertical test stand results in several ways: Contamination of the cavity during assembly, or relocation of dust particles when the cavity is measure in a horizontal rather than vertical position, may result in a deterioration of the achievable gradient. Differences in the detection of X-rays signalling field emission may result in changed limits from FE. Q_0 is not measured within the cryomodule, therefore the module tests results correspond more to the maximum than the "usable" gradient definition. Also, gradient measurements within Eu.XFEL modules were limited to 31.0 MV/m due to RF power limitations and to avoid any damage to cavities or input couplers, as no operation of cavities at Eu.XFEL at such high gradients is foreseen.

Comparing the measured average gradient in the cryomodule, which is cut off at 31.0 MV/m, to the vertical test results clipped to the same gradient, shows a 5.3 % gradient reduction to 28.5 from 30.1 MV/m for the maximum gradient and a 3.8 % gradient reduction to 27.5 from 28.6 MV/m comparing the operational to the usable gradient [52].

Cryomodule production data show that the performance difference between vertical test and module tests was larger for the first half of modules produced than for the second half. This correlates with a significantly improved production rate, where towards the end of production 1.25 modules were produced every week, i.e., one module every four days, more than the original target rate of 1 module per week. Numerous improvements were made during the course of cryomodule series production, resulting in faster turn around and better quality, as expected from learning curves.

Consequences of gradient spread: In order to increase the yield of usable cavities, a spread in usable gradient of ± 20 % around the mean value is accepted, for Eu.XFEL as well as ILC and LCF. This has important ramifications for operation: one klystron supplies 32 cavities at Eu.XFEL and 26 (full power) or 39 (low power) at ILC/LCF, and the RF power has to be distributed such that during operation cavities with reduced gradient do not surpass their gradient limit, while better performing cavities receive enough power to reach their operating gradient. At Eu.XFEL, the waveguide distribution system contains asymmetric shunt tees that are tailored prior to installation based on the cryomodule test results to achieve the desired RF distribution [53]. In contrast, the ILC design foresees remote controlled variable power splitters [1, Sect. 3.6.4], which are more expensive but add operational flexibility, making it possible to adjust the RF distribution based on the observed cavity performance in the beam. Thus, at ILC one can react to any changes in gradient limitations of individual cavities. This can be gradient reductions that would, for a fixed distribution, force a gradient reduction for a full klystron or detuning of the cavity, or improvements, e.g. from conditioning of the cavities. This design makes it possible to reduce the fraction of cryomodules tested from 100 % to 33 % once stable production performance has been established, and it will reduce the difference between gradients measured in the cryomodule tests and those achieved in actual beam operation.

The use of variable splitters is a mitigating measure to reduce performance risks arising from cavity performance degradation between cryomodule production and testing and actual operation with beam.

Performance in beam operation: As the largest operating accelerator facility based on TESLA technology, the European XFEL went into operation in 2017. It reached design energy on year later [54], despite the fact that only 97 cryomodules out of the planned 101 modules had been installed

and 21 cavities (2.7 %) of cavities were detuned, i.e., did not contribute to acceleration. 12 of the detuned cavities were functional, but at a reduced level, so that the performance penalty of detuning them was lower than operating all 32 cavities powered by the same klystron at reduced gradient. In the ILC design with variable splitters, these cavities could likely have been operated. Overall, the cavities reached 93.6 % of the performance measured in the module tests [54]. Comparisons between module test results and operation performance in beam show that on a cavity-by-cavity basis there is a sizeable (several MV/m) random difference between both results [54]. In the fixed, tailored power distribution system of Eu.XFEL the weakest cavity limits the operation of 32 cavities, costing several MV/m, an effect avoided by the ILC design.

The Eu.XFEL has remained in steady and successful operation, with excellent operating experience [55], see also Sec. 4.1.2 of [14]. It is due for its first warm up in the second half of 2025.

Operational experience from Eu.XFEL indicates that achieving an operational gradient in beam of 31.5 MV/m, i.e. 90 % of the gradient measured in vertical tests (5 MV/m) is challenging. Approximately 5 % gradient reduction are necessary as operation margin [56], thus only 5 % additional gradient reduction are acceptable.

Risk mitigation at LCF: The mitigation strategy of the LCF to cope with a situation where less than the nominal gradient is provided by the cavities has several components, and takes into account the differences in severity, depending on the actual amount of missing gradient.

For a Higgs factory with a nominal 250 GeV centre-of-mass energy, operation at 230 GeV (at a 8 % reduction of the gradient) would still yield valuable physics results. The yield characteristics of the undulator-based positron source, however, make it necessary to achieve at least 120 GeV beam energy for the electron beam, to avoid a severe impact on the physics programme. Therefore, at least 96 % of the nominal beam energy need to be available after commissioning to start physics operation, while it would be acceptable if it takes a couple of years (including the opportunity for technical interventions during shut downs) to reach 100 %.

The ILC and LCF baseline designs for 250 GeV foresee the installation of 837 cryomodules in the main linac, 423 (414) for the electron (positron) linac. Starting with an energy of 15 GeV after the two stage bunchg compressor, at the nominal gradient of 31.5 MV/m this would provide an end energy of 134.4 / 131.9 GeV; the larger energy in the electron linac accounts for the 3 GeV energy loss in the undulator for the positron source. Thus, the main linacs are designed with a 7 GeV or 6 % reserve. Operation of the main linac modules at 28.5 MV/m would thus result in beam energies of 123.0 / 120.8 GeV, enough to provide 240 GeV centre-of-mass energy and operate the positron source.

The LCF design for 550 GeV foresees 1881 (954 + 927) cryomodules, providing 284.3 / 276.7 GeV of beam energy. There is space for the installation of at least 9 + 45 more cryomodules, enough for 570 GeV centre-of-mass energy at nominal gradient.

The nominal operating gradient of 31.5 MV/m is the central estimate for the realistically achievable gradient in operation at LCF. A reserve of 6 % additional cryomodules is included in the design, and initial operation at 4 % lower gradient would be acceptable for physics operation, providing close to 10 % gradient reserve. The initial 250 GeV stage of LCF has ample tunnel space to raise the number of installed cryomodules, which makes it possible to revise the design even during the cryomodule production stage, after the performance of modules from series production has been measured.

This the risk mitigation strategy concerning the operational gradient consist of a 6 % reserve of installed cryomodules, and the option to re-assess the most cost-effective combination of operating gradient and number of installed cryomodules until late in the production and installation stage of the project, with small cost and schedule risk.

Cost impact of risk, cost opportunities: The assumption of a higher gradient for single cavities in vertical tests, compared to the Eu.XFEL production, is justified by a cavity overproduction of

11 %, requiring only 90 % yield, in contrast to a 0 % overproduction at Eu.XFEL, in conjunction with harder criteria for the re-treatment of cavities. This overproduction and the number of additional re-treatments and tests is included in the cost estimate. A future re-assessment of the expected gradient performance and yield might result in a revision of these parameters. Changing the yield from 90 % to 80 %, for instance, would increase the cavity production cost by 13 %. As cavities (including material) account for approximately half of the cryomodule costs, and cryomodules for a quarter of the project cost of LCF250, this would result in an overall project cost increase of less than 2 %. This cost risk is balanced by cost opportunities of comparable size: Eu.XFEL production data shows that a sizeable fraction of cavities shows gradient of 40 MV/m and more, thus the production yield could well be better than 90 %; further cost opportunities are given by the reduction of electro-polishing treatments from new surface treatments and because Eu.XFEL production experience shows that for most of re-treatments a cheap high-pressure rinse is sufficient instead of the EP step assumed in the costing.

A possible re-assessment of the realistic operating gradient, assumed to be 31.5 MV/m in the baseline design, would entail installation of more cryomodules together with more klystrons and modulators, and require and increased cryogenics capacity. Still, the complete SRF costs including cryogenics and HLRF entail 40 % of the total project cost, and thus a 10 % change of the assessed operating gradient would entail only a 4 % cost increase for the project overall.

8.2 Quality factor Q_0 and cryogenic power, new surface treatments

The ILC design parameters of 35 MV/m and $Q_0 = 1 \times 10^{10}$ in vertical tests have been the baseline since the publication of the TDR [1]; the staging report of 2017 [2] formulated a more optimistic R&D goal, raising the gradient by 10 % to 38.5 MV/m (35 MV/m in beam) and increasing Q_0 at the same time to 2×10^{10} (1.6×10^{10} in beam). Since the publication of these reports, significant progress has been made towards higher gradients and higher quality factors [14, Sect. 4.1.1]. In particular, the so–called mid–T bake surface treatment [57] followed by a low–T bake are promising, with single cell test results that already meet these targets [58], and successful industrialisation of these treatments in full cryomodules for SHINE [59]. In addition, mid–T / low–T baking offers further cost reduction opportunities, as it removes the need for a second electro-polishing (EP) step after the heat treatment, saving a cost intensive production step with a high environmental impact.

This progress is reflected in an LCF parameter set that assumes an quality factor of $Q_0 = 2 \times 10^{10}$, twice higher than the ILC baseline, at an unchanged target gradient, as a realistic estimate of the future state of the art. The 2017 R&D goal of achieving in addition gradient increase constitutes a further cost reduction opportunity beyond this central value.

In contrast to the onset of field emission or breakdown, gradient limitations due to Q_0 as included in the “usable” gradient definition of Eu.XFEL [19] does not constitute a hard limit for cavity operation. In fact, in module tests Q_0 is not even measured, and operating gradients are set by the hard limits [53], where Q_0 only enters if the degradation is so severe that a coupler power limit is reached.

Insofar, the nominal Q_0 target is predominantly a parameter that affects the estimate of the necessary cryogenic cooling capacity and the costs associated with this. The best estimate for a realistic performance can and will be reassessed after the R&D phase, at the start of procurement, and in the production phase when actual performance results from series production are available. Changes in the assessed average Q_0 value could result in changes of cryogenic plant dimensions or in the target operating gradient, or a combination of both.

The cost risk of changes to the cryogenic system is small: only 1/3 of the cryogenic power scales with $1/Q_0$, namely the losses in the cavity walls, while 2/3 are from other losses (static, losses in input couplers and HOM absorbers), and cryogenics contribute less than 10 % to the overall project cost for LCF250LP, ergo changing Q_0 back to 1×10^{10} would have only a 3 % impact on overall

project costs.

Overall, the risk associated with the Q_0 target is acceptable, and balanced by corresponding opportunities. The mitigation strategy in the design and production phase is a possible revision of gradient targets and/or cryo plant dimensions, with a small associated cost risk. In the operation phase, any unforeseen degradation of Q_0 would lead to a reduction of the pulse repetition frequency, associated with a reduction in luminosity, which is an acceptable performance risk that does not endanger the physics goals of the LCF.

8.3 Risk assessment conclusion

In summary, we assess that the ILC target gradient target for vertical tests of 35 MV/m at $Q_0 = 1 \times 10^{10}$ at a 90 % production yield, on which the cost estimate is based, has been demonstrated by Eu.XFEL production data to be the current state of the art of commercially available cavities. The LCF target of $Q_0 = 2 \times 10^{10}$ at the same gradient, production yield and cost is a realistic goal, based on R&D results for novel surface treatments, with significant opportunities for further performance increase and/or cost reduction.

The nominal target gradient of 31.5 MV/m for beam operation (90 % of the gradient in vertical tests), with at least 28.5 MV/m of gradient available after first commissioning, while not demonstrated in operational facilities, is a realistic performance goal. Equipping the RF distribution with variable power splitters will reduce the performance gap between module test and beam operation. A targeted R&D effort, starting with a careful analysis of experience from operating facilities such as Eu.XFEL, LCLS-II and others, will be required to deliver further improvements.

The performance goals given constitute our current best assessment of the performance realistically achievable by the time the project will be implemented, balancing remaining performance and cost risks and opportunities. These goals can and will be reassessed and possibly revised at various stages of the project, after the R&D phase, at placement of first orders, and during production. In particular, the LCF design facilitates an increase of the number of initially installed cryomodules. The design and production schedule of LCF offers enough flexibility for possible adjustments, which will not necessarily be for the worse, with minimal impact on schedule. The resulting cost impact is proportional to the assumed gradient change and is assessed to be no more than 10 % of the SRF system cost, which for LCF250LP would translate to 4 % of the overall project cost. Although not included in the cost uncertainty definition adopted by ILC and LCF, this cost risk is small compared the uncertainty for the SRF system (27 %) and the overall project (28 %). It does neither constitute a crippling project risk, nor is it a one-sided risk, but it is rather balanced by cost opportunities of comparable size.

Contributors and Supporters

C. Balazs
Monash University, Melbourne 3800 Victoria, Australia

G. Taylor
University of Melbourne, Victoria 3010, Australia

W. Mitaroff
Institute of High Energy Physics, Austrian Academy of Sciences, 1050 Vienna, Austria

A.H. Hoang, S. Plätzer
University of Vienna, Faculty of Physics, 1090 Vienna, Austria

M. Tytgat
Inter-University Institute for High Energies, Vrije Universiteit Brussel, 1050 Ixelles, Belgium

C. Hensel
Centro Brasileiro de Pesquisas Físicas, Rio de Janeiro 22290-180, Brazil

A.B. Bellerive
Carleton University, Ottawa, Ontario K1S5B6, Canada

F. Corriveau
Centre for High-Energy Physics, McGill University, Montreal, Quebec H3A2T8, Canada

D. Tuckler
TRIUMF, Wesbrook Mall, Vancouver, Canada

C.D. Fu, Q. Ouyang, H.R. Qi, M.Q. Ruan
Institute of High Energy Physics, Chinese Academy of Sciences, Beijing, China

I.P. Ivanov
Sun Yat-sen University, Guangzhou, Guangdong, China

M. Ouchemhou, T. Robens
Rudjer Boskovic Institute, 10000 Zagreb, Croatia

J. Cvach, J. Kvasnička, I. Polák, J. Zálešák
FZU - Institute of Physics of the Czech Academy of Sciences, 18200 Prague 8, Czechia

I.D. Gialamas, G. Hütsi, K. Kannike, A. Karam, L. Marzola, E. Nardi, J. Pata, A. Racioppi, M. Raidal
National Institute of Chemical Physics and Biophysics, 10143 Tallinn, Estonia

F. Djurabekova, K. Österberg
Helsinki Institute of Physics, University of Helsinki, 00014 Helsinki, Finland

E. Nagy, C. Vallee
Centre de Physique des Particules de Marseille, CNRS/IN2P3, Aix Marseille Université, Marseille, France

A. Arbey, G. Grenier, I. Laktineh, F. Mahmoudi
IP2I Institut de Physique des 2 Infinis CNRS/IN2P3, Université Claude Bernard, Lyon, France

D. Attié, M. Besançon, E. Cenni, P. Colas, N. Fourches, S. Ganjour, Z. Sun, M. Titov, B. Tuchming
Institut de recherche sur les lois fondamentales de l'Univers, CEA Saclay, 91191 Gif sur Yvette, France

J. Baudot
Université de Strasbourg, CNRS, IPHC UMR 7178, 67000 Strasbourg, France

F. Alharthi[0], P. Bambade, I. Chaikovska, R. Chehab, A. Faus Golfe, H. Guler, W. Kaabi, A. Korsun, F. LeDiberder, A. Martens, V.V. Mytrochenko[1], R. Pöschl, F. Richard, Y. Wang, M. Winter, X. Xia
IJCLab, Université Paris-Saclay, CNRS/IN2P3, 91405 Orsay, France

M.M. Altakach, S. Kraml
Laboratoire de Physique Subatomique et de Cosmologie, Université Grenoble-Alpes, CNRS/IN2P3, 38026 Grenoble, France

B. Fuks
Laboratoire de Physique Théorique et Hautes Energies (LPTHE), Sorbonne Université et CNRS, 75252 Paris, France

V. Boudry, J.-C. Brient, H. Videau
Laboratoire Leprince-Ringuet (LLR), École Polytechnique, 91128 Palaiseau, France

D. Zerwas
CNRS Helmholtz DMLab, Deutsches Elektronen-Synchrotron DESY, Hamburg, Germany

T. Behnke, M. Berggren, B. Bliewert, J. Braathen, K. Buesser, G. Eckerlin, M. Formela, F. Gaede, E. Gallo, N. Hamann, D. Käfer, K. Krüger, J. List, B. List, T. Madlener, V.I. Maslov, F. Meloni, M.T. Núñez Pardo de Vera, J. Reuter, S. Riemann, T Schörner, I. Schulthess, S. Spannagel, M. Stanitzki, J.M. Torndal, N. Walker, G. Weiglein[2], M. Wenskat, J.C. Wood
Deutsches Elektronen-Synchrotron DESY, Germany

L. Reichwein[3]
Forschungszentrum Jülich, Wilhelm-Johnen-Strasse, 52428 Jülich, Germany

B. Dudar
PRISMA+ Cluster of Excellence and Mainz Institute for Theoretical Physics, Johannes Gutenberg University, 55099 Mainz, Germany

U. Einhaus, M.M. Mühlleitner
Karlsruhe Institute of Technology, Karlsruhe, Germany

A. Caldwell, J. Farmer, W. Hollik
Max Planck Institute for Physics, 85748 Garching, Germany

P. Bechtle, C. Breuning, I. Brock, J. Kaminski, M. Lupberger, L. Reichenbach, M. Vellasco
University of Bonn, Physikalisches Institute, 53115 Bonn, Germany

N.M. Hartman
Technical University of Munich, Arcisstrasse 21, 80333 Munich, Germany

M. Boehler, S. Dittmaier, M. Schumacher
Physikalisches Institut, Albert-Ludwigs-Universität, Freiburg, Germany

M. Berger, M.V. Garzelli, G. Moortgat-Pick, M. Trautwein, A. Vauth
University of Hamburg, Hamburg, Germany

W. Kilian, T. Tong
Universität Siegen, 57068 Siegen, Germany

T. Ohl, W. Porod
Institute for Theoretical Physics and Astrophysics, University of Würzburg, 97074 Würzburg, Germany

A. Subba
Indian Institute of Science Education and Research Kolkata, Mohanpur, West Bengal, India

P. Poulose[4], A. Subba[5]
Indian Institute of Technology Guwahati, Assam 781039, India

N. Kumar
Shree Guru Gobind Singh Tricentenary University, Gurugram, Haryana 122505, India

J. Dutta
The Institute of Mathematical Sciences, CIT Campus, Tharamani, Chennai, Tamil Nadu, 600113, India

H. Abramowicz, Y. Benhammou, A. Levy
Tel Aviv University, Ramat Aviv 69978, Israel

S. Bilanishvili, M. Galletti, L. Verra, M. Zobov
INFN Laboratori Nazionali di Frascati, 00044 Frascati, Italy

M. Bertucci, E. Del Core, L. Monaco, R. Paparella, D. Sertore
INFN Sezione di Milano, 20133 Milano, Italy

E. Maina
Università degli Studi di Torino, Dipartimento di Fisica, 10125 Torino, Italy

C. Oleari
Università di Milano-Bicocca, 20126 Milano, Italy

K. Fujii, J. Fujimoto, A. Ishikawa, D. Jeans, Y. Kurihara, J. Nakajima, M. Nojiri, Y. Sakaki, T. Shidara, T. Tauchi, A. Yamamoto, M. Yamauchi
KEK, Tsukuba, Japan

T. Takahashi
Hiroshima University, Higashi Hiroshima, 739-8530, Japan

A. Das
Hokkaido University, Sapporo 060-0810, Japan

S. Yamashita
Iwate Prefectural University, Takizawa-city, Iwate, Japan

R. Hosokawa, K. Mawatari, S. Narita, M. Yoshioka
Iwate University, 4-3-5 Ueda, Morioka, Iwate, 020-8551, Japan

Y. Kato
Kindai University, 3-4-1 kowakae, Higashiosaka, Osaka, 577-8502, Japan

J. Maeda
Kobe University, 1-1 Rokkodai, Nada-ku, Kobe, 657-8501, Japan

T. Watanabe
Kogakuin Univeristy of Technology and Engineering, Shinjuku-ku, Tokyo 163-8677, Japan

K. Kawagoe, K. Tsumura
Kyushu University, 744 Motooka, Nishi-ku, Fukuoka, 819-0395, Japan

T. Chikamatsu
Miyagi Gakuin Women's University, Aoba-ku, Sendai, Japan

Y. Horii
Nagoya University, Nagoya, Japan

H. Ono
Nippon Dental University, Chuo-ku, Niigata 951-8580, Japan

Y. Seiya[6], K. Yamamoto[6]
Osaka Metropolitan University, Department of Physics, Osaka 558-8585, Japan

T. Takeshita
Shinshu University, Matsumoto, Nagano, Japan

K. Hamaguchi, Y. Iiyama[7], M. Ishino, S. Matsumoto[8], T. Mori, N. Nagata, W. Ootani, T. Suehara, J. Tian[7]
The University of Tokyo, Bunkyo-ku, Tokyo 113-0033, Japan

H. Yamamoto
Tohoku University, Aoba-ku, Sendai 980-8577, Japan

K. Hidaka
Tokyo Gakugei University, Koganei, Tokyo 184-8501, Japan

S. Hirose
University of Tsukuba, Tsukuba 305-8577, Japan

V.M. Bjelland
Norwegian University of Science and Technology, Trondheim, Norway

J. Kersten
Department of Physics and Technology, University of Bergen, 5020 Bergen, Norway

E. Adli, J.B.B. Chen, P. Drobniak, D.K Kalvik, C.A. Lindstrøm, F. Peña[9], K. Sjobak
Department of Physics, University of Oslo, 0316 Oslo, Norway

O.M. Ogreid
Western Norway University of Applied Sciences, 5020 Bergen, Norway

S.A. Khan
Dhofar University, Salalah, Oman

M. Idzik, J. Moron, A. Ukleja
AGH University of Krakow, Faculty of Physics and Applied Computer Science, 30-055 Kraków, Poland

M. Goncerz, M. Kucharczyk, T. Wojton
Henryk Niewodniczanski Institute of Nuclear Physics, Polish Academy of Sciences, Poland

M. Zielinski
Faculty of Physics, Astronomy and Applied Computer Science, ul. Lojasiewicza 11, 30-348 Krakow, Poland

B. Brudnowski, J. Kalinowski, J. Klamka, K. Mekala[10], A.F. Żarnecki, K. Zembaczynski
Faculty of Physics, University of Warsaw, Warsaw, Poland

I. Bozovic, I. Smiljanic, I. Vidakovic, N. Vukasinovic
Vinča Institute of Nuclear Sciences, University of Belgrade, Belgrade, Serbia

S.C. Park
Yonsei University, Seoul 03722, South Korea

O. Arquero, M.C. Fouz
Centro de Investigaciones Energéticas, Medioambientales y Tecnológicas (CIEMAT), Madrid, Spain

M. Almanza-Soto, C. Blanch, M. Boronat, J.C Fernandez-Ortega, J. Fuster, N. Fuster-Martínez, B. Gimeno, D. González-Iglesias, S. Huang, A. Irles, P. Martín-Luna, J.P. Márquez, D. Melini, A. Menéndez, V.A. Mitsou, M. Moreno-Llácer, E. Musumeci, C. Orero, L.K Pedraza-Motavita, G. Rodrigo, M. Villaplana, M. Vos, K. Wandall-Christensen
IFIC, CSIC-Universitat de València, Valencia, Spain

M. Fernandez, F.J. Gonzalez, R. Jaramillo, A. Lopez-Virto, D. Moya, A. Ruiz-Jimeno, I. Vila
Instituto de Física de Cantabria, IFCA, Santander 39005, Spain

T. Biekötter, S. Heinemeyer
Instituto de Física Teórica, CSIC-Universidad Autónoma de Madrid, Madrid, Spain

F.G. Celiberto
Universidad de Alcalá (UAH), Departamento de Física y Matemáticas, 28805 Alcalá de Henares, Madrid, Spain

J.L. Avila-Jimenez, J. Berenguer-Antequera, F. Cornet-Gomez
Universidad de Cordoba, Campus Universitario de Rabanales, 14071 Cordoba, Spain

D. Espriu
Universitat de Barcelona, Institut de Ciències del Cosmos, Barcelona 08028, Spain

F. Cornet, J. de Blas
Universidad de Granada, 18071 Granada, Spain

E.M. Donegani
European Spallation Source, 224 84 Lund, Sweden

J. Björklund Svensson
Department of Physics, Lund University, Lund, Sweden

M. Coman, M. Jacewicz, M. Olvegøard
Department of Physics and Astronomy, Uppsala University, Uppsala 752 37, Sweden

V. Cilento, R. Corsini, L.R. Evans, A. Latina, J. Osborne, S. Sasikumar, S. Stapnes, R. Tomás García, M. Williams
CERN, Geneva, Switzerland

T. Nakada
High Energy Physics Laboratory, Institute of Physics, Ecole Polytechnique Fédérale de Lausanne, 1015 Lausanne, Switzerland

M. Spira
Paul Scherrer Institut, 5232 Villigen, Switzerland

T.A. du Pree, P. Kluit, P. Koppenburg, J. Rojo, J. Timmermans, H. Wennlöf, S. Westhoff
Nikhef — National Institute for Subatomic Physics, Science Park 105, 1098 XG Amsterdam, The Netherlands

M. Mulder
Van Swinderen Institute, University of Groningen, Groningen, The Netherlands

H. Duran Yildiz
Institute of Accelerator Technologies, Golbasi 06830, Ankara, Türkiye

B. Bilki
Istanbul Beykent University, Istanbul, Türkiye

H. Denizli, A. Senol
Department of Physics, Bolu Abant Izzet Baysal University, 14280, Bolu, Türkiye

H. Sert
Department of Physics, Istanbul University, TR34134, Istanbul, Türkiye

L. Corner, T. Teubner
University of Liverpool, Liverpool L69 3BX, UK

E. Bulyak
National Science Center 'Kharkiv Institute of Physics and Technology', Kharkiv 61108, Ukraine

G. Burt
Lancaster University, Lancaster LA1 4YW, United Kingdom

C. Damerell, S. Easo
STFC Rutherford Appleton Laboratory, Chilton, Didcot OX11 0QX, United Kingdom

D. Angal-Kalinin, P.A. McIntosh, P.H. Williams
STFC Daresbury Laboratory, Keckwick Lane, Warrington WA4 4AD, United Kingdom

M. Wing[10]
Department of Physics and Astronomy, University College London, London WC1E 6BT, United Kingdom

N.K. Watson, A. Winter
School of Physics and Astronomy, University of Birmingham, Birmingham G15 2TT, United Kingdom

J. Goldstein
University of Bristol, Bristol BS8 1TL, United Kingdom

V.A. Khoze
University of Durham, Durham DH1 3DW, United Kingdom

V.J. Martin
University of Edinburgh, Edinburgh EH9 3FD, United Kingdom

A. Doyle, D. Protopopescu, A. Robson, Y. Zhang
University of Glasgow, Glasgow G12 8QQ, United Kingdom

R.B. Appleby, O. Apsimon, S. Boogert, R.M. Jones, V. Miralles
University of Manchester, Manchester M13 9PL, United Kingdom

P.N. Burrows, R. D'Arcy, B. Foster[10], D. Hynds, L. Kennedy[11]
University of Oxford, Oxford OX1 3RH, United Kingdom

K. Mimasu
University of Southampton, Southampton S017 1BJ, United Kingdom

F. Salvatore
University of Sussex, Brighton BN1 9QH, United Kingdom

K. Potamianos
University of Warwick, Coventry CV4 7AL, United Kingdom

S. Su
Department of Physics, University of Arizona, Tucson, AZ 85721, United States

G. Chen, C. Jing, R. Margraf-O'Neal, A. Ody, P. Piot, J.G. Power, J. Zhang
Argonne National Laboratory, Lemont, IL 60439, USA

B.F.L. Ward
Baylor University, Waco, TX 76798, USA

M. Liepe, J.R. Patterson
Cornell University, Ithaca, NY 14853, USA

A.V. Kotwal
Duke University, Durham, NC 27708, USA

S. Belomestnykh[12], L. Gray
Fermi National Accelerator Laboratory, Batavia, IL 60510, USA

R. Dermisek, R. Van Kooten
Department of Physics, Indiana University, Bloomington, IN 47405, USA

R.L. Geng, J. Grames, R.A. Rimmer, R. Ruber, A. Seryi
Jefferson Lab, Newport News, VA 23606, USA

E. Esarey, A. Formenti, C.G.R. Geddes, A.J. Gonsalves, T. Luo, A. McIlvenny, K. Nakamura, J. Osterhoff, S. Pagan Griso, A. Rastogi, S. Schroeder, C.B. Schroeder, D. Terzani, J. van Tilborg
Lawrence Berkeley National Laboratory, Berkeley, CA 94720, USA

A. Scheinker
Los Alamos National Laboratory, Los Alamos, NM, USA

X. Lu[13]
Northern Illinois University, DeKalb, IL 60115, USA

M. Demarteau, O. Hartbrich, F. Pilat
Oak Ridge National Laboratory, Oak Ridge, TN 37830, USA

S. Ampudia Castelazo, T. Barklow, A. Dhar, C. Emma, S. Gessner, M.J. Hogan, M. Kagan, N. Majernik, T.W. Markiewicz, S. Morton, E.A. Nanni, D. Ntounis, M.E. Peskin, J. Rabara Bailey, A. Schwartzman, D. Storey, C. Vernieri
SLAC National Accelerator Laboratory, Menlo Park, CA 94025, USA

P. Grannis, V.N. Litvinenko
Physics and Astronomy, Stony Brook University, NY 11794, USA

L. Reina
The Florida State University, Tallahassee, FL 32306, USA

K.T. Matchev
The University of Alabama, Tuscaloosa, AL 35487, USA

H.E. Haber
University of California, Santa Cruz, CA 95064, USA

M. Litos
University of Colorado Boulder, Boulder, CO 80309, USA

D. Bourilkov
University of Florida, Gainesville, FL 32611, USA

B. Bilki, Y. Onel, J.W. Wetzel
University of Iowa, Iowa City, IA 52242, USA

J. Anguiano, K. Kong, B. Madison, J.P. Ralston, C.S. Rogan, S. Rudrabhatla, G.W. Wilson
University of Kansas, Lawrence, KS 66045, USA

J.D. Wells
Physics Dept, Ann Arbor, MI 48109, USA

H. Baer
University of Oklahoma, Norman, OK 73019, USA

J.E. Brau, C.T. Potter, J. Strube
University of Oregon, Eugene, OR 97403, USA

K. Sugizaki
University of Pennsylvania, Philadelphia, PA 19104, USA

A.P. White
University of Texas at Arlington, Arlington, TX 76019, USA

Y. Bai, S. Dasu
University of Wisconsin–Madison, Madison, WI 53706, USA

[0]Also at: King Abdulaziz City for Science and Technology (KACST), Riyadh, Saudi Arabia
[1]Also at: NSC KIPT National Science Center "Kharkiv Institute of Physics and Technology" of The National Academy of Sciences of Ukraine, Kharkiv, Ukraine
[2]Also at: University of Hamburg
[3]Also at: Institute for Theoretical Physics I, Heinrich Heine University, Düsseldorf
[4]Also at: St. Joseph's University, Bangalore 560027, India
[5]Also at: Indian Institute of Science Education and Research Kolkata, Mohanpur, West Bengal, India
[6]Also at: Nambu Yoichiro Institute of Theoretical and Experimental Physics (NITEP)
[7]Also at: ICEPP
[8]Also at: Kavli IPMU
[9]Also at: Ludwig-Maximilians-Universität München, 85748 Garching, Germany
[10]Also at: Deutsches Elektronen-Synchrotron DESY, Germany
[11]Also at: CERN, Geneva, Switzerland
[12]Also at: Physics and Astronomy, Stony Brook University, NY 11794, USA
[13]Also at: Argonne National Laboratory, Lemont, IL 60439, USA

References

[1] *The International Linear Collider Technical Design Report - Volume 3.II: Accelerator Baseline Design* (2013), ed. by C. Adolphsen et al., arXiv: 1306.6328 [physics.acc-ph].

[2] L. Evans, S. Michizono, Linear Collider Collaboration, *The International Linear Collider Machine Staging Report 2017* (2017), arXiv: 1711.00568 [physics.acc-ph].

[3] Y. Abe et al., The International Development Team, *Status of the International Linear Collider* (2025), arXiv: 2505.11292 [hep-ex].

[4] A. Yamamoto et al., ILC-IDT Cost-update Task Force, *ILC250 Cost Update 2024 – Back-up Document to ESPPU submission No 275*, URL: https://indico.cern.ch/event/1439855/contributions/6461661/.

[5] J. Osborne, E. F. Mactavish, *Cost estimate for a LCF at CERN*, personal communication, 2025.

[6] I. Syratchev, *High efficiency klystron technologies*, Workshop on efficient RF sources, 2022, URL: https://indico.cern.ch/event/1138197/contributions/4821294/.

[7] F. Bordry et al., *Machine Parameters and Projected Luminosity Performance of Proposed Future Colliders at CERN* (2018), arXiv: 1810.13022 [physics.acc-ph].

[8] D. Delikaris, personal communication, 2025.

[9] G. Dugan, ILC Global Design Effort, *Guidelines for preparation of national cost estimates based on the ILC TDR value estimate*, 2013, URL: https://linearcollider.org/files/images/pdf/Costconversion%20report%20.pdf.

[10] *The Compact Linear Collider (CLIC) - Project Implementation Plan* (2018), ed. by M. Aicheler et al., DOI: 10.23731/CYRM-2018-004, arXiv: 1903.08655 [physics.acc-ph].

[11] S. Evans et al., ARUP Corp. *Life Cycle Assessment, comparative environmental footprint for future linear colliders CLIC and ILC*, 2023, URL: https://edms.cern.ch/document/2917948/1.

[12] S. Evans et al., ARUP Corp. *Life Cycle Assessment, comparative environmental footprint for future linear colliders CLIC and ILC, whole accelerator*, 2025, URL: https://edms.cern.ch/document/3283864/1.

[13] CERN, *CERN Environment Report 2021–2022*, 2023, DOI: 10.25325/CERN-Environment-2023-003.

[14] H. Abramowicz et al., Linear Collider Vision, *A Linear Collider Vision for the Future of Particle Physics* (2025), arXiv: 2503.19983 [hep-ex], URL: https://agenda.linearcollider.org/event/10624/program.

[15] IDT WG2, *ILC Technology Network (ITN) and work packages*, IDT-EB-2023-002, 2023, URL: https://linearcollider.org/wp-content/uploads/2023/09/IDT-EB-2023-002.pdf.

[16] T. Roser et al., *On the feasibility of future colliders: report of the Snowmass'21 Implementation Task Force*, JINST **18** (2023) P05018, DOI: 10.1088/1748-0221/18/05/P05018, arXiv: 2208.06030 [physics.acc-ph].

[17] T. Nakada et al., International Linear Collider International Development Team, *Proposal for the ILC Preparatory Laboratory (Pre-lab)* (2021), DOI: 10.5281/zenodo.4742043, arXiv: 2106.00602 [physics.acc-ph].

[18] U.S. Department of Energy, *Technology Readiness Assessment Guide*, DOE G 413.3-4A, 2015, URL: https://www.directives.doe.gov/directives-documents/400-series/0413.3-EGuide-04a-admchg1.

[19] D. Reschke et al., *Performance in the vertical test of the 832 nine-cell 1.3 GHz cavities for the European X-ray Free Electron Laser*, Phys. Rev. Accel. Beams **20** (2017) 042004, DOI: 10.1103/PhysRevAccelBeams.20.042004.

[20] N. Walker, *The European XFEL – experiences and lessons learnt*, 2017, URL: https://agenda.linearcollider.org/event/7645/contributions/39682/.

[21] D. Broemmelsiek et al., *Record High-Gradient SRF Beam Acceleration at Fermilab*, New J. Phys. **20** (2018) 113018, DOI: 10.1088/1367-2630/aaec57, arXiv: 1808.03208 [physics.acc-ph].

[22] G. Alexander et al., *Observation of Polarized Positrons from an Undulator-Based Source*, Phys. Rev. Lett. **100** (2008) 210801, DOI: 10.1103/PhysRevLett.100.210801.

[23] G. Alexander et al., *Undulator-Based Production of Polarized Positrons*, Nucl. Instrum. Meth. A **610** (2009) 451, DOI: 10.1016/j.nima.2009.07.091, arXiv: 0905.3066 [physics.ins-det].

[24] K. Yokoya et al., Positron Working Group, *Report on the ILC Positron Source*, 2018, URL: https://edmsdirect.desy.de/item/D00000001165115.

[25] G. Moortgat-Pick et al., *Prototypes and R&D for undulator-based positron sources*, EPJ Web Conf. **315** (2024) 02002, DOI: 10.1051/epjconf/202431502002.

[26] G. Moortgat-Pick et al., *R&D for positron sources at high-energy lepton colliders*, PoS **ICHEP2024** (2025) 841, DOI: 10.22323/1.476.0841.

[27] D. J. Scott et al., *Demonstration of a High-Field Short-Period Superconducting Helical Undulator Suitable for Future TeV-Scale Linear Collider Positron Sources*, Phys. Rev. Lett. **107** (17 2011) 174803, DOI: 10.1103/PhysRevLett.107.174803.

[28] H.-D. Nuhn, *LCLS Undulator Commissioning, Alignment, and Performance*, 31st International Free Electron Laser Conference, Proceedings of FEL2009, Liverpool, UK, 2009, 709 (THOA02), URL: https://accelconf.web.cern.ch/FEL2009/papers/thoa02.pdf.

[29] H.-S. Kang et al., *FEL performance achieved at PAL-XFEL using a three-chicane bunch compression scheme*, Journal of Synchrotron Radiation **26** (2019) 1127, DOI: 10.1107/S1600577519005861.

[30] S. Abeghyan et al., *First operation of the SASE1 undulator system of the European X-ray Free-Electron Laser*, J Synchrotron Radiat **26** (2019) 302, DOI: 10.1107/S1600577518017125.

[31] F. Dietrich et al., *Status of the undulator-based ILC positron source*, International Workshop on Future Linear Colliders, 2019, arXiv: 1902.07744 [physics.acc-ph].

[32] T. Lengler et al., *Characterization of radiation damages to positron source materials*, JACoW **IPAC2024** (2024) TUPC81, DOI: 10.18429/JACoW-IPAC2024-TUPC81.

[33] H. Nagoshi et al., *A design of an electron driven positron source for the internationallinear collider*, Nucl. Instrum. Meth. A **953** (2020) 163134, DOI: 10.1016/j.nima.2019.163134.

[34] M. Kuriki et al., *A design of ILC E-driven positron source*, JACoW **IPAC2022** (2022) WEPOPT023, DOI: 10.1088/1742-6596/2420/1/012006.

[35] A. Aryshev et al., *ATF report 2020* (2020), URL: https://cds.cern.ch/record/2742899/.

[36] A. Faus-Golfe et al., *ATF2-3 hardware upgrade and new experimental results to maximize luminosity potential of linear colliders*, Proc. IPAC'24 (Nashville, TN), IPAC'24 - 15th International Particle Accelerator Conference, 2024, 996 (TUPC04), DOI: 10.18429/JACoW-IPAC2024-TUPC04.

[37] M. Patecki et al., *Probing half β_y^* optics in the Accelerator Test Facility 2*, Phys. Rev. Accel. Beams **19** (2016) 101001, DOI: 10.1103/PhysRevAccelBeams.19.101001.

[38] R. J. Apsimon et al., *Design and operation of a prototype interaction point beam collision feedback system for the International Linear Collider*, Phys. Rev. Accel. Beams **21** (2018) 122802, DOI: 10.1103/PhysRevAccelBeams.21.122802, arXiv: 1812.08432 [physics.acc-ph].

[39] D. R. Bett et al., *High-resolution, low-latency, bunch-by-bunch feedback system for nanobeam stabilization*, Phys. Rev. Accel. Beams **25** (2022) 022801, DOI: 10.1103/PhysRevAccelBeams.25.022801, arXiv: 2201.01531 [physics.acc-ph].

[40] *Crab Cavity Design Review Meeting*, 2023, URL: https://agenda.linearcollider.org/event/10110/.

[41] *The International Linear Collider Technical Design Report - Volume 3.I: Accelerator R&D in the Technical Design Phase* (2013), ed. by C. Adolphsen et al., arXiv: 1306.6353 [physics.acc-ph].

[42] T. Naito et al.,
Multibunch beam extraction using the strip-line kicker at the KEK Accelerator Test Facility,
Phys. Rev. ST Accel. Beams **14** (2011) 051002,
DOI: 10.1103/PhysRevSTAB.14.051002.

[43] P. Tenenbaum et al.,
Emittance Preservation in the International Linear Collider Ring to Main Linac Transfer Line,
Proc. Particle Accelerator Conference (PAC 07), Albuquerque, New Mexico, 25-29 Jun 2007,
2007, 3118 (THPMS056), DOI: 10.1109/PAC.2007.4440687.

[44] K. Kubo, *Simulation of Low Emittance Transport in Long Straight Line of ILC RTML*,
ILC-NOTE-2007-008, 2007,
URL: https://edmsdirect.desy.de/item/D00000000954565.

[45] E.-S. Kim,
Control of emittance growth in a bunch compressor for the International Linear Collider,
IEEE Trans. Nucl. Sci. **56** (2009) 229, DOI: 10.1109/TNS.2008.2009117.

[46] P. Eliasson et al., *Study of an ILC main linac that follows the earth curvature*, Proc. 10th
European Particle Accelerator Conference (EPAC 06), Edinburgh, Scotland, 26-30 Jun 2006,
2006, 786 (MOPLS096),
URL: https://accelconf.web.cern.ch/e06/PAPERS/MOPLS098.PDF.

[47] K. Ranjan et al., *Emittance preservation for the curved ILC main linac*, Proceedings of 23rd
International Linear Accelerator Conference (LINAC06), Knoxville, TN, Aug. 21-25, 2006,
2006, 192 (MOP064),
URL: https://accelconf.web.cern.ch/l06/PAPERS/MOP064.PDF.

[48] *The International Linear Collider Technical Design Report - Volume 1: Executive Summary*
(2013), ed. by T. Behnke et al., arXiv: 1306.6327 [physics.acc-ph].

[49] H. Abramowicz et al.,
The International Linear Collider Technical Design Report - Volume 4: Detectors
(2013), ed. by T. Behnke et al., arXiv: 1306.6329 [physics.ins-det].

[50] A. Aryshev et al., ILC International Development Team,
The International Linear Collider: Report to Snowmass 2021 (2022),
arXiv: 2203.07622 [physics.acc-ph].

[51] W. Singer et al.,
Production of superconducting 1.3 GHz cavities for the European X-ray Free Electron Laser,
Phys. Rev. Accel. Beams **19** (2016) 092001,
DOI: 10.1103/PhysRevAccelBeams.19.092001.

[52] K. Kasprzak et al.,
Test Results of the European XFEL Serial-production Accelerator Modules,
18th International Conference on RF Superconductivity, 2018, MOPB106,
DOI: 10.18429/JACoW-SRF2017-MOPB106.

[53] S. Choroba, E. Apostolov, V. Katalev,
Series Production of the RF Power Distribution for the European XFEL,
28th International Linear Accelerator Conference, 2017, THPLR067,
DOI: 10.18429/JACoW-LINAC2016-THPLR067.

[54] D. Kostin et al., *SRF Operation at XFEL: Lessons Learned After More Than One Year*,
10th International Particle Accelerator Conference, 2019, MOYPLM2,
DOI: 10.18429/JACoW-IPAC2019-MOYPLM2.

[55] C. Schmidt et al., *Operational Experience with the European XFEL SRF Linac*, JACoW **SRF2023** (2023) MOIXA06, DOI: 10.18429/JACoW-SRF2023-MOIXA06.

[56] N. Walker, personal communication, 2025.

[57] S. Posen et al., *Ultralow Surface Resistance via Vacuum Heat Treatment of Superconducting Radio-Frequency Cavities*, Phys. Rev. Applied **13** (2020) 014024, DOI: 10.1103/PhysRevApplied.13.014024.

[58] L. Steder et al., *Further improvement of medium temperature heat treated SRF cavities for high gradients*, 2024, arXiv: 2407.12570 [physics.acc-ph].

[59] W. Pan et al., *High Q and high gradient performance of the first medium-temperature baking 1.3 GHz cryomodule*, Phys. Rev. Accel. Beams **27** (9 2024) 092003, DOI: 10.1103/PhysRevAccelBeams.27.092003.